Master Thesis

Design and demonstration of an automated gluing process for solar array manufacturing for space applications

University of Bremen
FB04 Faculty of Production Engineering

DLR Institute of Space Systems

Author:	Moritz Lahrmann
Matriculation Number:	6018097
First Examiner:	Dr. Ing. Andreas Rittweger
Second Examiner:	Sebastian Kottmeier
Submission Date:	19.06.2023

Universität Bremen

Deutsches Zentrum für Luft- und Raumfahrt
German Aerospace Center

Nachname **Lahrmann** Matrikelnr. **6018097**

Vorname/n **Moritz**

A) Eigenständigkeitserklärung

Ich versichere, dass ich die vorliegende Arbeit selbstständig verfasst und keine anderen als die angegebenen Quellen und Hilfsmittel verwendet habe.
Alle Teile meiner Arbeit, die wortwörtlich oder dem Sinn nach anderen Werken entnommen sind, wurden unter Angabe der Quelle kenntlich gemacht. Gleiches gilt auch für Zeichnungen, Skizzen, bildliche Darstellungen sowie für Quellen aus dem Internet.
Die Arbeit wurde in gleicher oder ähnlicher Form noch nicht als Prüfungsleistung eingereicht.
Die elektronische Fassung der Arbeit stimmt mit der gedruckten Version überein.
Mir ist bewusst, dass wahrheitswidrige Angaben als Täuschung behandelt werden.

B) Erklärung zur Veröffentlichung von Bachelor- oder Masterarbeiten

Die Abschlussarbeit wird zwei Jahre nach Studienabschluss dem Archiv der Universität Bremen zur dauerhaften Archivierung angeboten. Archiviert werden:

1) Masterarbeiten mit lokalem oder regionalem Bezug sowie pro Studienfach und Studienjahr 10 % aller Abschlussarbeiten
2) Bachelorarbeiten des jeweils ersten und letzten Bachelorabschlusses pro Studienfach u. Jahr.

- [x] Ich bin damit einverstanden, dass meine Abschlussarbeit im Universitätsarchiv für wissenschaftliche Zwecke von Dritten eingesehen werden darf.
- [ ] Ich bin damit einverstanden, dass meine Abschlussarbeit nach 30 Jahren (gem. §7 Abs. 2 BremArchivG) im Universitätsarchiv für wissenschaftliche Zwecke von Dritten eingesehen werden darf.
- [ ] Ich bin nicht damit einverstanden, dass meine Abschlussarbeit im Universitätsarchiv für wissenschaftliche Zwecke von Dritten eingesehen werden darf.

C) Einverständniserklärung über die Bereitstellung und Nutzung der Bachelorarbeit / Masterarbeit / Hausarbeit in elektronischer Form zur Überprüfung durch Plagiatssoftware

Eingereichte Arbeiten können mit der Software *Plagscan* auf einen hauseigenen Server auf Übereinstimmung mit externen Quellen und der institutionseigenen Datenbank untersucht werden.
Zum Zweck des Abgleichs mit zukünftig zu überprüfenden Studien- und Prüfungsarbeiten kann die Arbeit dauerhaft in der institutionseigenen Datenbank der Universität Bremen gespeichert werden.

- [x] Ich bin damit einverstanden, dass die von mir vorgelegte und verfasste Arbeit zum Zweck der Überprüfung auf Plagiate auf den *Plagscan*-Server der Universität Bremen hochgeladen wird.
- [ ] Ich bin ebenfalls damit einverstanden, dass die von mir vorgelegte und verfasste Arbeit zum o.g. Zweck auf dem *Plagscan*-Server der Universität Bremen hochgeladen u. dauerhaft auf dem *Plagscan*-Server gespeichert wird.
- [ ] Ich bin nicht damit einverstanden, dass die von mir vorgelegte u. verfasste Arbeit zum o.g. Zweck auf dem *Plagscan*-Server der Universität Bremen hochgeladen u. dauerhaft gespeichert wird.

Mit meiner Unterschrift versichere ich, dass ich die oben stehenden Erklärungen gelesen und verstanden habe. Mit meiner Unterschrift bestätige ich die Richtigkeit der oben gemachten Angaben.

Datum Unterschrift

Abstract

The Deutsches Zentrum für Luft- und Raumfahrt(German Aerospace Center) (DLR) aims to manufacture solar panels for their individual space missions. To increase flexibility and decrease costs a collaborative robot is used in this process. An important step in this process is the bonding of the fragile solar cells to a larger supporting structure with an adhesive.

The adhesive bond for the connection of the solar cells to the supporting structure was developed, based on the expected loads and environment encountered during the lifetime of the solar array. The selected adhesive for this bond is the silicone adhesive Wachker RTV 691.

A process for the application and the bonding of the solar cells was created. This process utilizes the collaborative robot and uses differed developed tools. For the application of the adhesive a tool is used that compresses a syringe with a stepper motor and a connected screw drive. The solar cells are handled by a tool that lifts them up by utilizing a vacuum.

Further tests were performed to verify if the process can fulfill the requirements. A replacement adhesive had to be used for these tests. A definitive answer if this was successful, could therefore not be given, but the results look promising. This process could be used to manufacture 1 W of solar array power every 28.5 s.

Contents

List of Figures

List of Tables

Nomenclature

Symbols

E	young's modulus
k	bulk modulus
m	mass
$\dot{m}$	mass flow
t	time
V	volume
v	velocity
$\dot{v}$	acceleration
α	thermal expansion coefficient
μ	shear modulus
ν	poisson's ratio
ω	rotational velocity
φ	volume ratio

Indices

0	at time 0
A	in axial/ fibre direction
a	in axial direction
bot	of the robot
ext	of the extruder
f	of the fibre
L	of the laminate

l	in lateral direction
M	mean value
m	of the matrix
$step$	of the stepper motor
T	in transverse direction
t	at time t
$total$	in total

List of Acronyms

ATOX Atomic Oxygen

BoL Begin of Life

CFRP Carbon-fiber-reinforced plastic

DLR Deutsches Zentrum für Luft- und Raumfahrt(German Aerospace Center)

GEO Geostationary orbit

GFRP Glass-fiber-reinforced plastic

LEO Low Earth orbit

PLC Programmable Logic Controller

RTV-1 Room Temperature Vulcanizing Silicone 1-component

RTV-2 Room Temperature Vulcanizing Silicone 2-component

UD unidirectional

1. Introduction

Solar panels are an essential part of every satellite. They provide the necessary power for the operation of the satellite and therefore it is essential that the they can be flexible designed and manufacture to fit the need of every mission and satellite. They usually consist of multiple individual solar cells that are bonded to a larger structure. The DLR seeks to develop a process for the flexible manufacturing of different solar panels to fit the need of their different missions. The goal of this these is to develop a gluing process, that can connect a string of multiple solar cells to a larger structure. In this process a collaborative robot is utilized to automate parts of this process while maintaining a degree of flexibility.

In chapter 2 the problem is described in more detail. In the following chapter 3 further theoretical background knowledge is given. The design process is described in chapter 4. The resulting designs are described in chapter 5. Chapter 6 describes the different experiments that were performed and chapter 7 describes the designed bonding process. The results are discussed and further recommendations are given in the chapters 8.

2. Problem Description

The DLR designs and builds satellites for scientific missions. These missions often require satellites with a non standard design. For example they are often smaller than the large commercial communication satellites. Therefore they often need solar panel that have an uncommon size or design. To reduce the cost for these solar arrays a flexible semi automated manufacturing process should be developed.

Towards this goal a welding process was already developed, that electrically connects multiple solar cells together to a string of ten cells in one line. In another step these cell strings shall now be bonded to a larger supporting structure. Figure 2.1 shows the basic design of such a solar array. The adhesive connects the thin cell string (only 5 in one line are shown in the figure 2.1) to a much larger and stronger supporting structure. This adhesive layer has to support all the expected loads and environmental conditions the solar array is subjected to in its lifetime. In this these a adhesive for this application has to be selected and the parameters of this adhesive layer have to be defined.

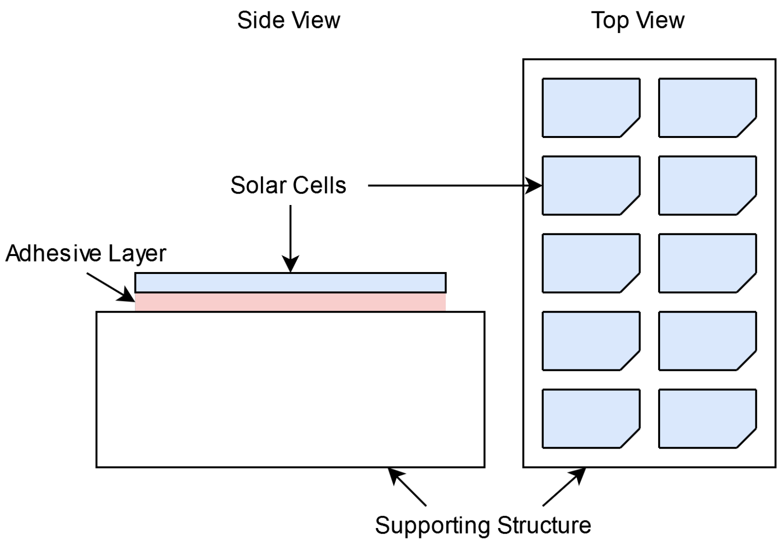

Figure 2.1.: diagram of a simplistic example solar array (not to scale)

For the creation of this bond the adhesive has to be applied to the supporting structure in a consistent amount and in a pattern that does not interfere with the space environment. The cell strings have to be picked up from their welding position, where they lay face down. The have to be turned face up and placed on top of the adhesive and a contact pressure has to be applied to them to spread the adhesive and ensure a good wetting of the surfaces by the adhesive. This process has to be repeatable and consistent to guarantee a sufficient quality of the final product.

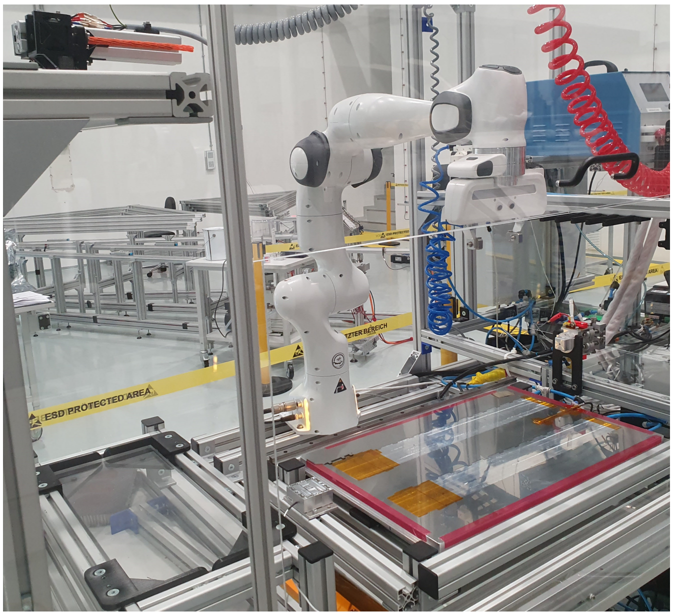

Figure 2.2.: picture of the workspace with robot

The picture 2.2 shows the workspace with the robot. The structure is placed in the bottom left corner of the image. The welding position, from where the cell strings have to be lifted up, is located in the bottom left corner and marked with red tape in this picture.

For the amortization of such processes normally industrial robots are used, but they are usually limited to large scale series production, due to there low flexibility and high acquisition cost. This makes robots hard to utilize in the spacecraft integration process, which only comprises of prototypes or small scale series. To mitigate these problems a collaborative robot is utilized, which enables the cooperation between robot and operator. This increases the flexibility of the system by profiting of the high versatility of the human worker.

3. State of the Art

3.1. Solar Arrays

Solar Arrays are the main source of electrical power for most spacecraft. They convert a portion of the solar radiation into usable electrical energy. This energy is stored in batteries for later use during the eclipse phase. Solar arrays usually consist of multiple Cells connected in series to strings and bypass diodes mounted to some surface. In spin stabilized satellites they are usually mounted directly to the spacecraft body, while on 3-axis stabilized satellites they mounted to a support structure [1]. In general the cells are connected to the structure by using a silicone adhesive [2]. On most modern Spacecraft the solar cells used are Gallium Arsenide based. They have multiple advantage over the traditionally used Silicon based cells. They are more suitable for the operation in thermally demanding environments and are also more resistant to strong radiation. Another advantage of these cells is that multiple layers can be placed on top of each other, where each layer is specialised in a specific spectral frequency range. This Multi-junction solar cells can reach a higher efficiency compared to single layer cells [3].

3.2. Robot Human Collaboration

The industrial robot is a commonly used machine in the series manufacturing of many products, for example cars. But it is rarely used in the manufacturing of small scale series or prototype production, like for example the spacecraft production. This is caused by the high investment cost of these robot systems. Usually the robot itself is only responsible for one quarter of the cost, the other part is the mechanism for the provision of the base material and the custom tools necessary for each task. These investments are specific to a certain task done by the robot and can not be repurposed for other tasks the robot might be able to perform. Therefore these investments are only feasible when the robot performs the same task many times, which is only the case for large scale series productions [4].

A possible solution for this problem is the close integration of humans and robots together in the manufacturing process. In this Robot Human Collaboration both parts can use their strengths. The use of a human in the process makes the system more flexible and easier to adapt to different tasks [4].

This interaction between human and robot also causes new problems especially in regards to safety. In the traditional application of industrial robots, the robots and the humans are strictly separated, but this prohibits any form of interaction between them. A possible solution is to separate the work area and limit the movement and speed of the robot in the area where interaction with humans happens. Another way to reduce the risk is to limit the moved mass. These light-weight robots have a high ratio between robot mass and load capacity, of up to 2:1. This, together with a limited load mass, reduces the overall mass that needs to be moved and limits the kinetic energy of the system. In new systems this is combined with contact sensors to register collisions and safely stop the robot and prevent squeezing. An example for such a system is the Robot "Panda" from "Franka Emika" [4].

3.3. Adhesion and Adhesives

This section gives an overview about the fundamental working principles of adhesive. It also describes the basic properties of different types of adhesives to help in the design of the adhesive bond.

3.3.1. Definitions

Adhesion: Adhesion is the attraction of two different material to each other, as a result of molecular forces [5].

Cohesion: Cohesion describes the acting of attraction forces in between atoms and molecule of the same material. In the context of adhesive bonds, it is often used to describe the internal strength of the adhesive [6].

Adhesive: Is a material which, when applied to the surfaces of two material can join them together and resist separation [5].

Substrates: The materials which shall be bonded together are called substrates [5]

Adherent: After bonding substrates are generally called adherent [5].

Primer: A primer is a substance which is applied to the surface of at least one substrate to improve the adhesion or protect the surface [5].

Interface: The interface is the plane of contact in between adhesive and adherent [5].

Pot-Life: Is the time after the mixing of all adhesive components that can be used for the processing of the adhesive [6].

3.3.2. Theory of Adhesion

The phenomenon of adhesion on a fundamental level is caused, by different mechanisms, which dependent on the materials and conditions play a larger or smaller roll. Therefore, a universal theory of adhesion does not exist. The primary mechanisms for adhesion are described in different theories, but all have in common, that the both material have to come into close contact with each other this is called wetting [2], [5].

3.3.2.1. Adsorption Theory

In the adsorption theory bonding forces act between to materials on a molecular level as soon as they come into contact with each other. These bonding forces are chemical in nature and one or more of the following bonding forces can be the origin of these forces dependent on the materials used [2], [5].

Covalent Bond Is the main type of bond between atoms of non metals. This bond is created by the sharing of valence electrons between atoms. This is the primary bond in organic chemistry which includes most types of adhesives [2].

metallic bond Is the main type of bond between atoms of metals. This bond is created by the free flowing electrons in the metal lattice. This electrons can act into the boundary layer between adhesive and metal and interact with the molecules and atoms of the adhesive [2]. This bond together with the covalent bond is stronger than the following inter molecular forces [6].

Dipole Forces Some molecules with atoms with a large difference in electronegativity form a permanent electric dipole moment. This has a attracting and directing influence on neighboring dipole molecules. This dipole moments can effect other material, especially metals. If a dipole molecule is close to a metal it can polarise it and therefore create an attraction force between metal and adhesive. This is the reason why adhesives with dipole molecules connect especially good to metals [2].

Induction Forces A dipole can be induced into an otherwise unpolar molecule, if a part of it is substituted by a part with a strong electron attracting or repelling character. The resulting induction forces tend to be smaller than the dipole forces [2].

Dispersion Forces In a dipole-less molecule the random movement of the electrons can temporary create a small dipole. This can in return induce a dipole in the neighboring molecules. This interaction between molecules leads to attraction forces between them, but these forces tend to be smaller than the previously described dipole forces [2].

Hydrogen bond The hydrogen bond is a special type of bond between a molecule with a strong positively charged hydrogen atom and another molecule with a negative part. The hydrogen bonded to the strong electronegative atom, usually a OH or NH, is positively charged. The resulting attraction forces between the hydrogen atom an the negative part of the other molecule is especially high, because the molecules can come into very close contact with each other due to the small size of the hydrogen atom [2].

3.3.2.2. Mechanical Theory

The mechanical theory describes adhesion as a result of the liquid glue filling in microscopic pores, undercuts or similar structures on the rough surface of the adherent. After the hardening this creates a form closure between the adherent and the solid glue. This type of adhesion is important for materials with a porous surface, while for materials with a smooth surface its influence on the total adhesion is small [2], [6].

3.3.2.3. Electrostatic Theory

In the electrostatic theory the interface between adhesive and adherent is described as the two plates of a capacitor. This theory is based on the existence of small amounts of free electric charges in all solid materials, even in dielectrics. These charges tend to move across the interface between the materials due to the difference in electrochemical potential. This creates an electric double layer, which helps to connect the two substances by electrostatic forces. The extend and importance of these force is disputed [5].

3.3.2.4. Diffusion Theory

Diffusion is the spontaneous mixing of two substances, which are in contact with each other. The diffusion theory focuses on polymers and describes, that the molecules of both substances diffuse into the other substance and the interface becomes less defined over time until it vanishes. This process is most prominent in the gluing of polymers with a solvent which liquefies the surfaces and allows for the mixing of the molecules from both substrates. Afterwards the solvent will evaporate from the joint and leaves the molecules locked together [5], [6].

3.3.3. Adhesive Types

3.3.3.1. Reactive Adhesives

This adhesive is applied while it is still a liquid to wet the substrates, afterward it sets an becomes a solid. In this type of adhesive the setting is caused by a chemical reaction. The reaction is dependent on different external influences like temperature and humidity [6].

Epoxides Epoxides are two component adhesives. In generally they have a high mechanical strength but a low ductility and are one of the most common industrial adhesives. Compared to other organic adhesive they have a high resistance to chemicals and temperature, but still should not be heated above 140 °C. They are usually sold as two components which have to be mixed prior to application in a precise ratio. There also exist some products which are premixed, but the chemical reaction is thermally blocked. This adhesives have to be heated up to start the reaction but the shelf life of this products is limited [6].

Anaerobic Adhesives Anaerobic adhesives are single component adhesives that react if they come into contact with certain metals even under the exclusion of air. They can only be applied in very thin layers and are primarily used for screw and bolt connection [6].

Cyanoacrylates Cyanoacrylates are single component solvent free adhesives, with a short reaction time. They also have a high mechanical strength and are brittle. For the hardening reaction water acts as an initiator and catalyst. The water on the surface of the adherents from the air humidity is enough for this reaction. But this limits the thickness of the adhesive to a maximum of 0.2 mm If the relative humidity is below 30% the reaction might be limited or impossible. On the other hand if the humidity is to high the reaction might happen to fast which might result in a very brittle adhesive layer. They can also be damaged by high temperatures and should not be subjected to temperatures above 70 °C [6].

Polyurethanes Polyurethanes can be single as well as two component adhesives. In the single component variant the adhesive reacts with the water in the air, this limits the area that can be glued together, if no water can diffuse through the adherents. The one component version usually has a lower mechanical strength, but is ductile even at low temperatures. While the two component version is less ductile, it has a high mechanical strength. A major risk when working with polyurethane adhesive is the production of isocyanates during the hardening process. They can range dependent on the exact chemical composition from an irritant to very toxic [6].

Silicone Silicone are inorganic adhesives that can either use one or two components. The one component, often called Room Temperature Vulcanizing Silicone 1-component

(RTV-1), reacts with the moisture in the air. This makes them easy to handle and apply, but water has to defuse through the adhesive for a complete reaction. This exponentially increases the reaction time dependent on the adhesive thickness and limits the area that can be glued. Also RTV-1 silicone tend to shrink during the curing process. The two component variant, often called Room Temperature Vulcanizing Silicone 2-component (RTV-2), has a much shorter reaction time and the adhesive thickness is not limited by the water diffusion, but the application process is more complicated especially because silicon tends to dissolve a lot of air during the mixing process, which can cause bubbles if the pressure decreases rapidly. In general silicone has a very low mechanical strength but has a large maximum elongation. It is also very temperature resistant with a normal range from $-50\,^{\circ}\mathrm{C}$ to $150\,^{\circ}\mathrm{C}$. Special types can even reach a range from $-100\,^{\circ}\mathrm{C}$ to $-250\,^{\circ}\mathrm{C}$. It is also very resistant to chemical and environmental degradation [6]. Another advantage of silicone compared to the organic adhesives is its resistance to Atomic Oxygen (ATOX) which is very common in the low earth orbit [7].

3.3.3.2. Hot-meld Adhesives

This adhesive can be melted for the application and wetting of the adherents. It solidifies when it cools down and by this develops its final strength. The advantage of this adhesive is its time until it reaches full strength and its lack of toxic fumes or solvents. It's short work time can also be a disadvantage especially when working with metals, because it might cause the adhesive to cool down to far before the other substrate can be correctly positioned. In this case preheating of the parts might be necessary. Another property of this type of adhesive is that the binding process is reversibly by heating. This can be an advantage if the parts should be separable but also cause a low resistance to high temperature, because the adhesive loses its strength long before it melts. There also exist mixed forms with reactive adhesive that are applied in a molten form but not only physically solidify but also chemically react. This type is not reversible but is more tolerant towards high temperatures [6].

3.3.3.3. Solvent Based Adhesives

In this type the adhesive is dissolved in a solvent that after application diffuses out of the joint. This requires that the solvent can leave the joint, so the substrates have to be permeable for the solvent. Therefore they can not be used for metals. Also the adhesive shrinks during the solidifying process and the resulting adhesive has a low strength. Organic solvents often cause additional problems, because they are often flammable and toxic [6].

3.3.3.4. Pressure Sensitive Adhesives

This is a single component adhesive which is permanently sticky. They are applied to one surface, while being either melted or dissolved. Afterward they start setting on this surface and become a very high viscose sticky liquid. They can stay this way for an extended period of time. To form an adhesive bond another object has to be pressed into the adhesive. The quality of the connection is in direct relation to the applied pressure, because the pressure causes the wetting. The primary application for this type of adhesives are adhesive tapes. They have the advantage, that they are easy to use and already have a good adhesion directly after application. They have the disadvantage that the supported maximum loads are lower compared to other adhesive types and that they tend to creep more, because they are still a liquid [6].

4. Design Process

This chapter describes the design process for the adhesive bond as well as for the bonding process. It describes the different functions and resulting requirements the adhesive bond and the bonding process have to fulfill. It also describes and analyses the other influences on the design and there effect on the design parameters. Finally it lists the different options for the implementation and gives advantages and disadvantages for both.

4.1. Design Parameters

The design of the adhesive bond and the bonding process is influenced by different parameters. This includes already selected parts for the solar array as well as environmental influences or operating conditions.

4.1.1. Robot

The robot used for these tasks is the lightweight robot "Panda" from "Franka Emika". It has 7-axis and can handle masses up to 3 kg. It is equip with sensors for the measuring of forces and torques. It has a measuring accuracy of at least 0.8 N. These sensors also allows the robot to detect collisions in under 2 ms, which enables the collaboration with a humans worker without endangering them. This force sensing capability also allows the robot to precisely apply forces in different directions. The robot can also be equipped with different end effectors. In this case it is equipped with the devise called "Hand" which has two fingers it can use to grab different objects [8]. With this the robot can grab onto a part of the additional tools called "Tool Interface".
The robot is installed in a box made of acrylic glass and aluminium extrusions. This box protects the working area and especially the welding process from airflow and resulting temperature fluctuations.
The manufacturer provides two different options for the control of the robot. One option is the browser based graphical programming interface called "DESK". In this program the different basic function the robot can perform, like movement, are blocks called apps and they can be placed after each other to be executed in this order to create more complex task. This options has the advantage, that it is easy to use, but it is limited to the available apps. It also does not support variables or different coordinates systems

for the work piece or tool. This makes the process inflexible. The other option is the "Franka Control Interface" which allows the control of the robot by C-code and uses the connected computer as a the controller for the robot. This gives direct access to the low-level functions like direct control of the individual motors and sensors of the robot [8]. This allows for a flexible control of the robot, but all higher level functions have to be build up from scratch, which is out of scope for this thesis.

The robot is used in this application, because it already comes with a lot of built-in functionalities, like for example force sensing. this allows for the design of more simple tools, which are faster and cheaper to manufacture. Its ability to detect collisions allows it to work in close proximity to a human operator, without the presence of disruptive safety features like fences. In this application it allows the operator to work closely with the robot. The operator can for example prepare the next welding process, while the robot applies the adhesive for the cell strings.

4.1.2. Solar Cells

The solar cells used for this solar panel are the "Triple Junction GaAs Solar Cell Type: TJ Solar Cell Assembly 3G30A" with an external silicon bypass diode from Azur Space. Such a cell is depicted in figure 4.1.

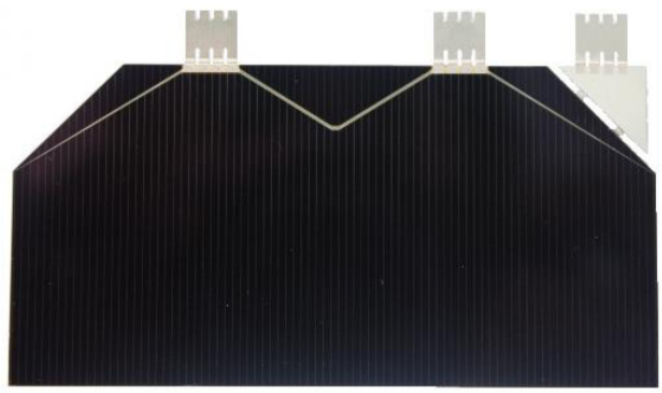

Figure 4.1.: picture of a Solar Cell Assembly 3G30A (source: [9])

This cells cover an area of 40.15 mm x 80.15 mm, but one corner is cut off resulting in an area off 30.18 cm^2. They have a thickness of 280 µm and a mass per area of 118 $mg\,cm^{-2}$ [9]. This results in a total mass of 3.56 g. They also have three interconnectors on one end, which are thinner and they will be spaced 2 mm apart in this solar panel. Electrically they produce at the Begin of Life (BoL) a peak voltage of 2409 mV and a peak current of 502.9 mA [9].

4.1.3. Support Structure

It is planed to manufacture the supporting structure for the solar panel in the DLR, but at the time of writing no prototype has been build jet. Figure 4.2 shows the planed structure.

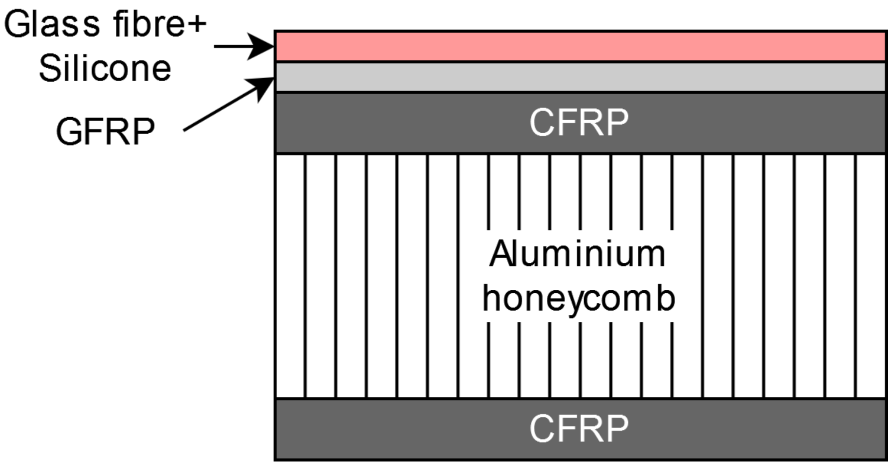

Figure 4.2.: support structure

This planed structure uses an aluminium honeycomb with a thickness of 20 mm and a honey comb cell size of 1/4in as the core and at the top and bottom it has a layer of Carbon-fiber-reinforced plastic (CFRP). The honeycomb is a "PMAG -XR1-1.6-1/4-0007-P-5056". The CFRP layer itself should be made up of 3 layers of $[+45/-45]_s$ carbon fibre in a epoxies matrix. On top of this is a single layer of Glass-fiber-reinforced plastic (GFRP) as an electrical insulator and again on top of this as a protection against ATOX a layer of glass fibre in silicone. Both glass fibre layers also use $[+45/-45]_s$ laminates. At the time of writing the exact thickness of these layers is still unknown.

4.1.4. Mechanical Loads

A spacecraft experiences the highest mechanical loads during the launch in the form of the rockets acceleration and vibration. Therefore the adhesive bond has to support the weight of the solar cells for the maximum possible acceleration. Also the orientation of the solar panel relative to the rocket is unknown therefore the worst possible orientation has to be assumed. For an adhesive bond the worst load case would be a bending torque which starts peeling of the adhesive. If only forces are applied the worst case would be a shear force.

As an example for the expected acceleration and vibration, data from the SpaceX Falcon9 User guide is used. In this guide the expected maximal acceleration in axial and lateral direction is given for a small spacecraft, below 1815 kg. The maximum total acceleration is at an axial acceleration of 8.5g and a lateral acceleration of 2g. The maximum acceleration due to vibration is give with 0.9g in axial direction and 0.6g in lateral direction [10]. Together this results in an axial acceleration of $92.2\,\mathrm{m\,s^{-2}}$ and a lateral acceleration of $25.5\,\mathrm{m\,s^{-2}}$.

$$\dot{v}_{total} = \sqrt{\dot{v}_a^2 + \dot{v}_l^2} \tag{4.1}$$

By using the equation 4.1 a total load of acceleration of $95.7\,\mathrm{m\,s^{-2}}$. This accelerations only cause forces and not bending torques, because they are not rotational. The worst case therefore is an acceleration and resulting force parallel to the adhesive plane like shown in figure 4.3.

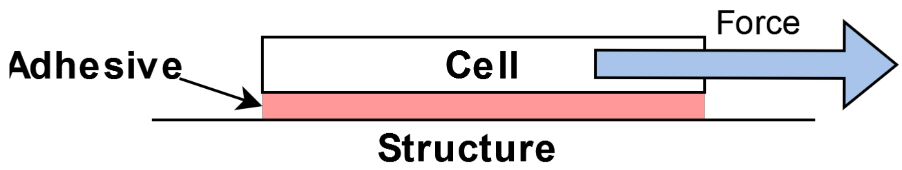

Figure 4.3.: mechanical load: worst case direction

The expected force is not only dependent on the acceleration, but also on the mass of the cells. The mass of a single cell is 3.56 g (see section 4.1.2). Therefore the resulting force is 0.34 N. If a safety factor of 3 is applied to account for some additional force, perhaps due to a different launch vehicle, the resulting force is still only 1 N.

4.1.5. Temperature

A spacecraft receives heat from different sources. The important heat inputs are the internal heat dissipation from the electrical equipment, the radiation from the sun and if orbiting a body the respective albedo and planet shine. In most cases this is earth. Furthermore these inputs varies a lot over time and are dependent on the selected orbit and spacecraft geometry [1]. Therefore any temperature range requirement without a given orbit and spacecraft design can only be a very broad estimation and should later be checked against the real mission and spacecraft design.

In "Thermal analysis of composite solar array subjected to space heat flux" the authors numerically simulate a solar panel in Low Earth orbit (LEO) and Geostationary orbit (GEO). They use a similar panel design with a honeycomb support panel a cover layer of GFRP and solar cells on top. In their simulation the highest and lowest points are reached at the edges at the end of the solar panel furthest from the spacecraft. But a more representative point for the temperature of the adhesive is in the center of the panel. In the LEO the highest temperature in the center is 380 K and the lowest temperature is 242 K. In the GEO the simulated temperature in the center ranges from 180 K up to 350 K [11]. Therefore a temperature range of 180 K up to 380 K is assumed for the solar panel in this thesis. With an additional margin of error of 20 °C a temperature range from −115 °C up to 125 °C is required.

4.1.6. Thermal Expansion

An important function of the adhesive layer is to offset the difference in thermal expansion between the supporting honeycomb structure and the solar cells. This directly influences the required elasticity of the adhesive and the thickness of the adhesive layer. For this the temperature range and thermal expansion coefficient of both the cells and the support structure have to be known.

4.1.6.1. Thermal Expansion of the Solar Cell

The manufacturer of the solar cells does not provide a thermal expansion coefficient , but the total thickness of the cells and the cover glass is known. The glass has a thickness of 100 µm and the total thickness of the cell is 280 µm [9]. Therefore it can be assumed that the GaAs substrate has a thickness of 180 µm.

GaAs has a thermal expansion coefficient α of $5 \cdot 10^{-6}\,\mathrm{K}^{-1}$ at room temperature [12] and a young's modulus E of 82 GPa [13]. Optical glasses have a thermal expansion coefficient at room temperature in between $7.6 \cdot 10^{-6}\,\mathrm{K}^{-1}$ and $8.4 \cdot 10^{-6}\,\mathrm{K}^{-1}$ [14]. Glass also has a young's modulus of around 60 GPa at room temperature [15]. If we assume that the cells are perfectly rigid in shear and do not bend the total thermal expansion can be calculated by the equations of mixing:

$$E_{total}\alpha_{total} = \varphi_1 E_1 \alpha_1 + \varphi_2 E_2 \alpha_2 \tag{4.2}$$

$$E_{total} = \varphi_1 E_1 + \varphi_2 E_2 \tag{4.3}$$

The volume ratio φ is the result of the ratio between the thickness of both layers. For the glass $\varphi = \frac{5}{14}$ and for the GaAs $\varphi = \frac{9}{14}$. If using the above stated values the resulting total young's modulus is 74.1 GPa. With this and a thermal expansion coefficient of $8 \cdot 10^{-6}\,\mathrm{K}^{-1}$ for the glass the resulting total thermal expansion coefficient is $5.87 \cdot 10^{-6}\,\mathrm{K}^{-1}$.

4.1.6.2. Thermal Expansion of the Support Structure

For the support structure the thermal expansion of the different layers is first calculated separately. The following equations are given in [16] for an composite unidirectional (UD) layer.

$$E_A \alpha_A = V_f E_A^f \alpha_A^f + V_m E_A^m \alpha_A^m + 2\lambda(\nu_A^m - \nu_A^f)\varphi_f \varphi_m [\alpha_T^m + \nu_A^m \alpha_A^m - \alpha_T^f + \nu_A^f \alpha_A^f] \quad (4.4)$$

$$\begin{aligned} \alpha_T + \nu_A \alpha_A = {} & (\alpha_T^f + \nu_A^f \alpha_A^f)\varphi_f + (\alpha_T^m + \nu_A^m \alpha_A^m)\varphi_m \\ & + \frac{\lambda}{2}\left(\frac{1}{k_T^f} - \frac{1}{k_T^m}\right)\varphi_f \varphi_m [(\alpha_T^m + \nu_A^m \alpha_A^m) - (\alpha_T^f + \nu_A^f \alpha_A^f)] \end{aligned} \quad (4.5)$$

$$E_A = \varphi_f E_A^f + \varphi_m E_A^m + 2\lambda(\nu_A^m - \nu_A^f)\varphi_f \varphi_m \quad (4.6)$$

$$\frac{1}{\lambda} = \frac{1}{2}\left[\frac{1}{\mu_T^m} + \frac{\varphi_f}{k_T^m} + \frac{\varphi_m}{k_T^f}\right] \quad (4.7)$$

$$\frac{1}{k_T} = \frac{2(1-\nu_T)}{E_T} - \frac{4\nu_A^2}{E_A} = \frac{\varphi_f}{k_T^f} + \frac{\varphi_m}{k_T^m} - \frac{\lambda}{2}\left(\frac{1}{k_T^f} - \frac{1}{k_T^m}\right)\varphi_f \varphi_m \quad (4.8)$$

$$\mu_T = \varphi_f \mu_T^f + \varphi_m \mu_T^m - \lambda_1 \left(\mu_T^f - \mu_T^m\right)^2 \varphi_f \varphi_m \quad (4.9)$$

$$\frac{1}{\lambda_1} = \varphi_m \mu_T^f + \varphi_f \mu_T^m + \frac{k_T^m \mu_T^m}{k_T^m + 2\mu_T^m} \quad (4.10)$$

$$\frac{1}{E_T} = \frac{\nu_A^2}{E_A} + \frac{1}{4}\left(\frac{1}{k_T} + \frac{1}{\mu_T}\right) \quad (4.11)$$

$$\nu_T = \frac{E_T}{2\mu_T} - 1 \tag{4.12}$$

$$\mu_A = \varphi_f \mu_A^f + \varphi_m \mu_A^m - \lambda_2 \left(\mu_A^f - \mu_A^m\right)^2 \varphi_f \varphi_m \tag{4.13}$$

$$\frac{1}{\lambda_2} = \mu_A^f \left(1 + \varphi_f\right) + \mu_A^f \varphi_m \tag{4.14}$$

All the above equations are only valid for a single UD layer. The following equations from [16] give the young's modulus and thermal expansion coefficient for a $[+\theta/-\theta]_s$ laminate. This is a symmetrical laminate and θ gives the angle between the x-axis and the fibre direction.

$$\alpha_2(\theta) = \alpha_2(-\theta) = \alpha_A \cos^2\theta + \alpha_T \sin^2\theta \tag{4.15}$$

$$\alpha_3(\theta) = \alpha_3(-\theta) = \alpha_T \cos^2\theta + \alpha_A \sin^2\theta \tag{4.16}$$

$$\alpha_4(\theta) = -\alpha_4(-\theta) = (\alpha_A - \alpha_T)\sin 2\theta \tag{4.17}$$

$$g_{22}(\theta) = g_{22}(-\theta) = \left(\frac{1}{\mu_A} - \frac{2\nu_A}{E_A}\right)\cos^2\theta\sin^2\theta + \frac{\cos^4\theta}{E_A} + \frac{\sin^4\theta}{E_T} \tag{4.18}$$

$$g_{24}(\theta) = -g_{24}(-\theta) = -\cos\theta\sin\theta\left[\left(\frac{1}{\mu_A} - \frac{2\nu_A}{E_A}\right)\cos 2\theta - \frac{2\cos^2\theta}{E_A} + \frac{2\sin^2\theta}{E_T}\right] \tag{4.19}$$

$$g_{33}(\theta) = g_{33}(-\theta) = \left(\frac{1}{\mu_A} - \frac{2\nu_A}{E_A}\right)\cos^2\theta\sin^2\theta + \frac{\cos^4\theta}{E_T} + \frac{\sin^4\theta}{E_A} \tag{4.20}$$

$$g_{44}(\theta) = g_{44}(-\theta) = \left(\frac{1}{E_A} + \frac{1}{E_T} + \frac{2\nu_A}{E_A}\right) sin^2 2\theta + \frac{\cos^2 2\theta}{\mu_A} \tag{4.21}$$

$$\frac{1}{E_A^L(\theta)} = g_{22}(\theta) - \frac{g_{24}^2(\theta}{g_{44}(\theta} \tag{4.22}$$

$$\alpha_A^L(\theta) = \alpha_2(\theta) - \frac{g_{24}}{g_{44}}\alpha_4(\theta) \tag{4.23}$$

For $\theta = 45°$ the following is valid $E_A^L(45°) = E_T^L(45°)$ and $\alpha_A^L(45°) = \alpha_T^L(45°)$. This holds true for the selected laminates in the support structure (see section 4.1.3) which are all $[+45/-45]_s$.
The exact materials of the support structure are still unknown. Therefore representative values for the chosen materials are used, these have to be later adjusted, when the real properties are known.
For the epoxied matrix the following values are used [16]:

- $E_A = E_T = 4.05\,\mathrm{GPa}$;young's modulus
- $\mu_A = 1.5\,\mathrm{GPa}$;shear modulus
- $\nu_A = \nu_T = 0.35$;poisson's ratio
- $\alpha_A = \alpha_T = 5 \cdot 10^{-5}\,\mathrm{K}^{-1}$;thermal expansion coefficient

For the silicone matrix the following values are used [17]:

- $E_A = E_T = 0.024\,\mathrm{GPa}$;young's modulus
- $\mu_A = 0.01\,\mathrm{GPa}$;shear modulus
- $\nu_A = \nu_T = 0.48$;poisson's ratio
- $\alpha_A = \alpha_T = 2.75 \cdot 10^{-4}\,\mathrm{K}^{-1}$;thermal expansion coefficient

For the glass fibre the following values are used [16]:

- $E_A = E_T = 75\,\mathrm{GPa}$;young's modulus
- $\mu_A = 30\,\mathrm{GPa}$;shear modulus
- $\nu_A = \nu_T = 0.25$;poisson's ratio
- $\alpha_A = \alpha_T = 5 \cdot 10^{-6}\,\mathrm{K}^{-1}$;thermal expansion coefficient

For the glass fibre the following values are used [16]:

- $E_A = 200\,\mathrm{GPa}$;axial young's modulus
- $E_T = 15\,\mathrm{GPa}$;transverse young's modulus
- $\mu_A = 18\,\mathrm{GPa}$;shear modulus
- $\nu_A = 0.25$;axial poisson's ratio
- $\nu_A = 0.35$;transverse poisson's ratio

- $\alpha_A = -1 \cdot 10^{-6}\,\mathrm{K}^{-1}$;transverse thermal expansion coefficient
- $\alpha_T = 2 \cdot 10^{-5}\,\mathrm{K}^{-1}$;transverse thermal expansion coefficient

Table 4.1 shows the young's modulus and thermal expansion coefficients calculated with the equations from 4.4 to 4.23 and the above stated material properties. A fibre volume fraction of 50% was assumed.

Table 4.1.: support structure layer properties

Layer type	E_L	α_L
CFRP	13.156 GPa	$4.35 \cdot 10^{-6}\,\mathrm{K}^{-1}$
GFRP	12.411 GPa	$1.91 \cdot 10^{-5}\,\mathrm{K}^{-1}$
silicone + glass fibre	0.1195 GPa	$5.59 \cdot 10^{-6}\,\mathrm{K}^{-1}$

The honeycomb is made out of aluminium with a young's modulus of 70 GPa. The honeycomb has a cell size of $h = 1/4inch$ and a wall thickness of $t = 0.0007inch$. In SI units this is $h = 6.35\,\mathrm{mm}$ and $t = 0.017\,78\,\mathrm{mm}$. Figure 4.4 shows a schematic of a honeycomb core with the important parameters marked.

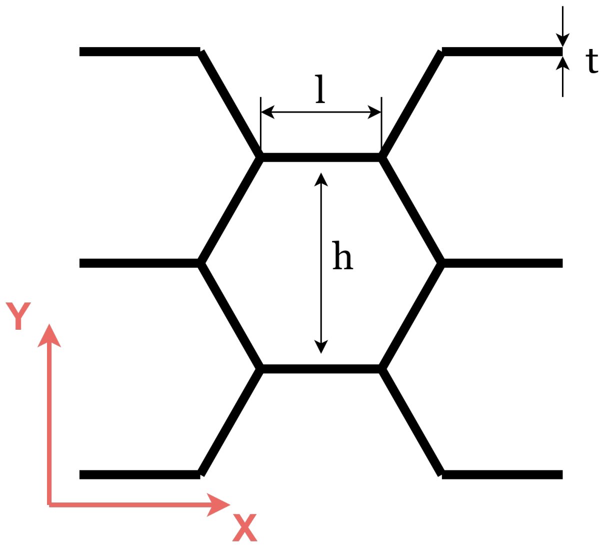

Figure 4.4.: honeycomb schematic

The wall length l can be calculated to 3.67 mm by the following equation:

$$l = \frac{h}{2\cos 30^\circ} \tag{4.24}$$

The young's modulus in the x and y direction can be calculated by the following equations [11]:

$$E_x = \frac{4\sqrt{3}}{3} E_{solid} \left(\frac{t}{l}\right)^3 \left[1 - 3\left(\frac{t}{l}\right)^2\right] \tag{4.25}$$

$$E_y = \frac{4\sqrt{3}}{3} E_{solid} \left(\frac{t}{l}\right)^3 \left[1 - \frac{5}{3}\left(\frac{t}{l}\right)^2\right] \tag{4.26}$$

With these equations and the parameters of the honeycomb the young's modulus can be calculated to $E_x = 1.8438 \cdot 10^{-5}\,\mathrm{GPa}$ and $E_y = 1.8439 \cdot 10^{-5}\,\mathrm{GPa}$. These values are a lot smaller than the calculated values for the fibre composite layers $E_{honeycomb} << E_{CFRP}$. Therefore it is assumed that the influence of the honeycomb core on the thermal expansion in the plane is limited and can be neglected.

For the calculation of thermal expansion of the support structure the equation 4.3 and 4.2 are used. For the volume ratio φ the ratio of the layers is used: $\varphi_{CFRP} = \frac{6}{8}$, $\varphi_{GFRP} = \frac{1}{8}$, $\varphi_{silicone+fibre} = \frac{1}{8}$. This results in a total young's modulus of $E_{total} = 11.433\,\mathrm{GPa}$ and a thermal expansion coefficient of $\alpha_{total} = 6.353 \cdot 10^{-6}\,\mathrm{K}^{-1}$.

4.1.6.3. Layer Thickness

The adhesive has to full fill a similar function to a sealant. It has to offset the different thermal expansion of the solar cells and the supporting structure. The adhesive has to elongate in the way shown in figure 4.5.

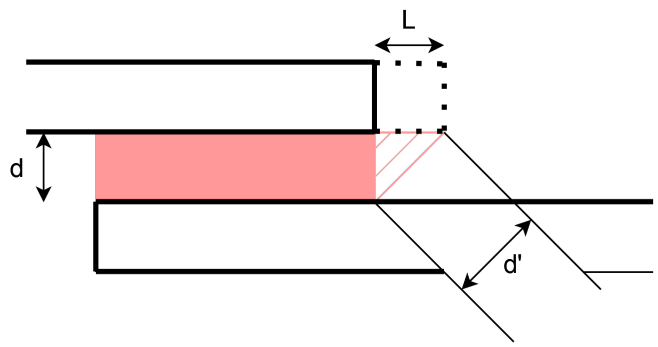

Figure 4.5.: adhesive elongation

The difference in length L can be calculated from the difference in thermal expansion from the section 4.1.6.1 and 4.1.6.2 $\alpha_{cell} = 5.87 \cdot 10^{-6}\,\mathrm{K}^{-1}$, $\alpha_{structure} = 6.353 \cdot 10^{-6}\,\mathrm{K}^{-1}$ and the maximum length over which such a change can occur. In this case this length is the diagonal of the solar cell (see section 4.1.2) with a height of 40.15 mm and a width of 80.15 mm. The length of this diagonal l is 89.64 mm. Also relevant s the maximum difference in temperature ΔT of 240 K (see section 4.1.5). The difference in length L can be calculated with the following equation:

$$L = l\,(\alpha_{cell} - \alpha_{structure})\,\Delta T \tag{4.27}$$

This results in length L of 0.01 mm. The relation ship between the elongation ϵ and the thickness d of the adhesive layer is described by the following equation [5]:

$$d' = \sqrt{L^2 + d^2} \tag{4.28}$$

$$\epsilon = \frac{d' - d}{d} \tag{4.29}$$

With this the minimum adhesive layer thickness can be calculated dependent on the maximum elongation of the adhesive. If the maximum elongation is 80% ($\epsilon_{max} = 0.8$) the minimum layer thickness d has to be 0.007 mm. This is below the minimum layer thickness that can be practically manufactured. It can also be observed, that the load carrying capacity for bonds is reduced for thicknesses below 0.1 mm,because the wetting of the surfaces is limited [2]. Therefore the adhesive should have a minimum thickness of 0.1 mm

4.2. Functions

4.2.1. Adhesive Bond Functions

The adhesive bond has to fullfil different functions in this assembly. Figure 4.6 shows the function tree for the adhesive bond, which gives an overview about this different functions.

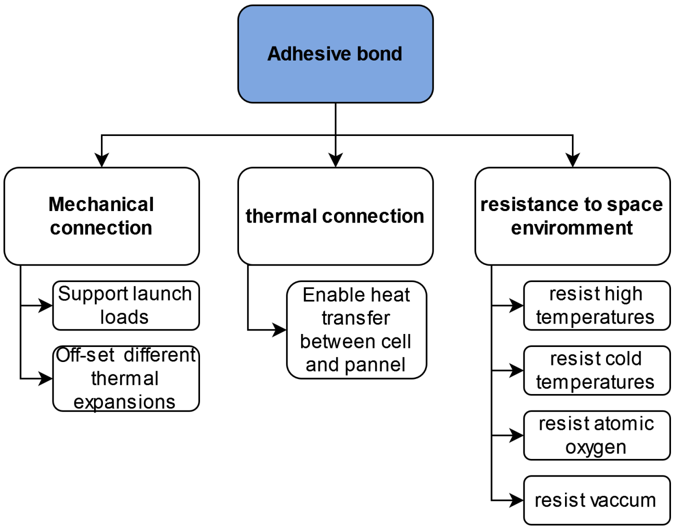

Figure 4.6.: function tree: adhesive bond

4.2.1.1. Mechanical Connection

The adhesive has to provide a mechanical connection between the solar cells and the supporting CFRP sandwich panel. This connection has to support the mechanical loads during the launch, which are caused by the acceleration and the vibrations. The adhesive also has to compensate for the different thermal expansion of the cells and the CFRP sandwich panel, because the cells and the supporting panel have different coefficients of thermal expansion and they also might have different temperatures.

4.2.1.2. Thermal Connection

The adhesive also has to thermally connect the CFRP panel and the solar cells. If the solar panel is in the sun light the adhesive has to transport the heat from the front of the panel to the backside, where it can be radiated to reduce the temperature of the cells. If the solar panel is in the shadow it has to connect it to the thermal mass of the CFRP sandwich panel so they don't cool down to quickly. The thermal connection is also important to reduce the difference in temperature between the solar cells and the CFRP sandwich panel to reduce the difference in thermal expansion described in the previous section.

4.2.1.3. Resistance to Space Environment

The adhesive has to survive the harsh space environment with only limited degradation during its lifetime. Therefore it has to tolerate the expected high and low temperatures. Another environmental hazard for the adhesive is the vacuum and if the solar panel is used in LEO it additionally has to withstand the constant interaction with ATOX.

4.2.2. Bonding Process Functions

The process of applying the adhesive and bonding the cells to the supporting CFRP panel has to fulfill m multiple functions shown in Figure 4.7.

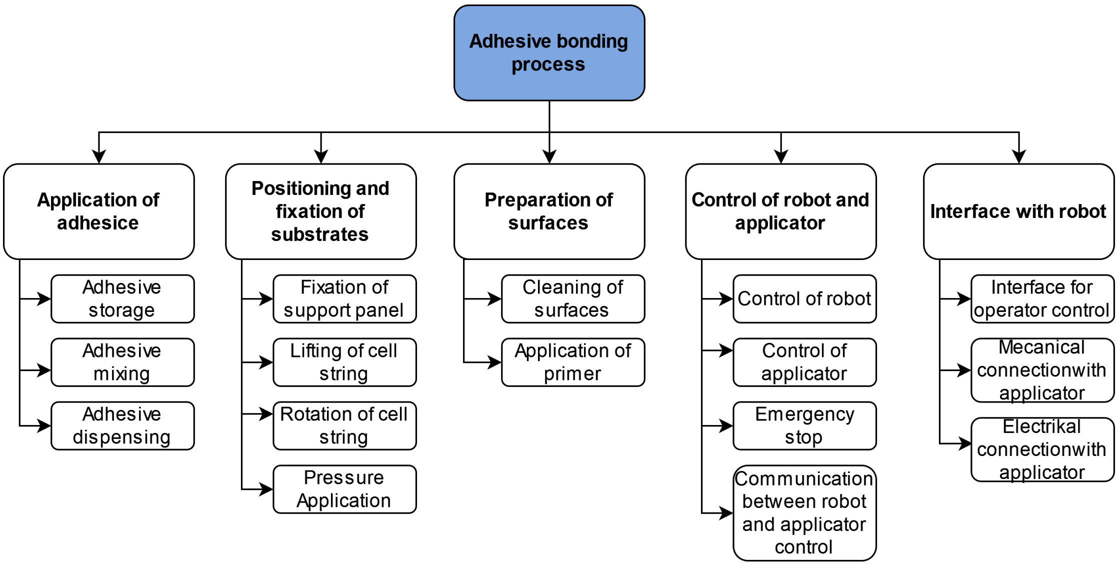

Figure 4.7.: function tree: bonding process

4.2.2.1. Adhesive Application

If a two component adhesive is used, it has to be mixed in the correct ratio prior to the application process. It also has to be stored until is it applied to one of the substrates. Finally the adhesive has to be applied to one of the substrates at the right location in the right amount.

4.2.2.2. Substrate Positioning

For the application of the adhesive at least one of the substrates has to be fixed in place at a precise position so the adhesive can be applied in the correct position. Also the other substrate has to be moved from a pick up position onto the other surface and placed there in the correct position. Finlly pressure has to be applied to the substrates to press them together, which in turn spread the adhesive and fixes them in place.

4.2.2.3. Surface Preparation

Before the application of adhesive can start the surfaces of the substrates have to be prepared. They have to be cleaned and then a primer has to be applied to the surfaces if necessary.

4.2.2.4. Robot and Applicator Control

The motion of the robot and adhesive application tool has to be controlled. This includes the positioning of the robot and the application of adhesive. The robot and application tool also have to communicate to synchronise with each other. Also both robot and applicator has to stop in an emergency.

4.2.2.5. Interfaces

For the operation of the robot in has to interface with different parts in different ways. The Operator has to be able to control the robot therefore a human robot interface is necessary. Also the robot has to interface with the tools mechanically to support the operational loads. Finally the robot has to interface with the tools electrically to enable a communication between both as described in the previous section.

4.3. Requirements

4.3.1. Adhesive Bond Requirements

Table 4.2 shows all the requirements for the adhesive bond. The column "Requirement text" shows the full text of the requirement. The column "Origin" shows where the requirement originated, parent requirements are just shortened to "Rq" plus the number of the requirement. If the requirement originates in a different part of this thesis, the section or figure is listed. For example figure 4.6 refers to function tree: adhesive bond. The column "Verification" lists by what method the requirement can be verified.

Table 4.2.: requirements: adhesive bond

No.	Requirement text	Origin	Verification
1.	The solar cells and the support structure shall be mechanically connected under all expected operational conditions and during the expected lifetime of the system.	figure 4.6	Test
2.	The adhesive bond of structure and solar cells shall support the launch loads without damage (at least 1 N per cell).	figure 4.6, Rq1, section 4.1.4	Test
3.	The adhesive shall compensate for the different thermal expansions of the solar cells and the structure.	figure 4.6, Rq1, section 4.1.5	Test
4.	The maximum elongation of the adhesive shall be at least 80%.	Rq3, section 4.1.6.3	Test
5.	The adhesive between the substrates shall have a thickness off 0.25 mm +/- 0.15 mm	Rq2, Rq3, section 4.1.6.3	Test
6.	The adhesive shall be able to withstand the space environment in LEO and GEO orbits	figure 4.6	Demonstration
7.	The adhesive shall withstand temperatures and keep its flexibility in a range from $-115\,°C$ up to $125\,°C$	Rq6, section 4.1.5	Test
8.	The adhesive shall be resistant to atomic oxygen	Rq6	Demonstration
9.	The adhesive shall be low out gassing in accordance to ECSS-Q-ST-70-02	Rq6	Test

4.3.2. Process and Application System Requirements

The table 4.3 lists all the requirements for the process of applying the adhesive and bonding the structure and the cells. It also show the origin of the requirement and the verification method similar to table 4.2.

Table 4.3: requirements: process and application system

No.	Requirement text	Origin	Verification
11.	The process shall be reproducible.		Demonstration
12.	The application system shall apply the adhesive to one of the substrates.	figure 4.7	Demonstration
13.	The application system shall supply the adhesive in the required condition as defined by the supplier.	figure 4.7	Demonstration
14.	The application system shall temporarily store enough adhesive for 2 solar cell strings of 10 cells each.	figure 4.7	Demonstration
15.	The application system shall be able to at least store 0.5 mL of adhesive per cell.	Rq14	Demonstration
16.	The application system shall dispense enough adhesive for each solar cell	figure 4.7	Demonstration
17.	The application system shall dispense at least 0.5 mL of adhesive per solar cell	Rq16	Test
18.	The application system shall dispense the adhesive at a uniform rate	Rq11	Test
19.	The application shall provide the adhesive without the inclusion of air	Rq6	Demonstration
20.	The adhesive application pattern shall prevent the formation of air pockets inside the adhesive bond	Rq6	Demonstration
21.	The solar cells and the structure shall not be damaged in the process		Demonstration
22.	The panel structure shall be fixed in place for the process	figure 4.7	Demonstration
23.	The cell handling system shall be able to lift and move a welded string of 10 solar cells from the welding to the gluing position	figure 4.7	Demonstration
24.	The solar cell string shall be rotated 180° along its longest axis	figure 4.7	Demonstration
25.	The solar cells shall be pressed onto the surface of the panel structure with a force of 20 N +/- 5 N per cell	Rq21	Test
26.	All glued surfaces shall be cleaned beforehand	figure 4.7	Demonstration
27.	Primer shall be applied to the surface of the structure beforehand	figure 4.7	Demonstration

Continued on next page

Table 4.3: requirements: process and application system (Continued)

28.	The system shall work together with the Franka-Panda robot		Demon-stration
29.	The application tool shall connect mechanically with the robot	figure 4.7	Demon-stration
30.	The cell handling tool shall connect mechanically with the robot	figure 4.7	Demon-stration
31.	The robot shall be able to automatically change between the different tools		Demon-stration
32.	The operator shall be able to select different programs for the robot	figure 4.7	Demon-stration
33.	The controller for the application system shall be able to communicated with the robot controller and vice versa	figure 4.7	Demon-stration
34.	All power shall be cut to the robot and applicator if the emergency stop is activated	figure 4.7	Demon-stration

4.4. Trade-Offs

4.4.1. Adhesive Selection

For the application on a space solar array the most important properties of an adhesive are its heat resistance, flexibility and long-time durability even under the harsh space conditions like vacuum and UV-radiation. In the space environment the adhesive has to have a high resistance to the extreme temperatures. It must be able to survive the high temperatures in the sun ight for an extended period of time without degrading. It must also resist the cold temperatures without losing its flexibility to still be able to compensate for the different expansion of cell and support structure. The adhesive must also keep its characteristics even after a long period of time in these conditions. Table 4.4 gives an overview of the most important adhesive properties and how the different types compare against each other.

Table 4.4.: overview Adhesive advantageous (+) and disadvantageous properties (source: [6])

	Epoxide	Anaerobic adhesives	Cyano-acrylates	Polyure-thanes	Silicone	Hot-meld adhesives
price	+	0	-	0	0	+
toxicity	+	+	0	-	+	+
pot life	0	+	-	-	+	+
mechanical strength	+	+	+	+	-	+
flexibility	-	0	-	+	+	+
heat resistance	+	0	-	-	+	-
long term durability	0	0	-	+	+	0

Silicone is the optimal type of adhesive under these requirements. It can withstand high temperatures of over 200 °C without degrading and special types of silicone stay flexible even at extremely low temperatures. It also is has a good longtime durability especially under UV radiation compared to most other adhesives. Another big advantage of silicone over all the other organic based adhesives it is resistance to ATOX, which would severely damage all other adhesives that are exposed to it. A small advantage for the manufacturing process is, that silicone and its base components are not toxic and therefore no special precautions have to be taken when working with it. Silicone biggest disadvantage is its low mechanical strength. All other adhesives are able to support more load, but this disadvantage is less important in this application. The mass of the solar cells is very low and therefore all the expected loads are also very low (see: section 4.1.4). Silicone is available in a one component (RTV-1) or two component (RTV-2) form. The RTV-1 has the advantage of an easy application process, but would increase the time needed for the curing. It also needs the moisture from the air for its curing process, but the solar cells are impermeable to water and the area is to large for water to diffuse from the sides into the joint. Therefore RTV-2 has to be used, which cures faster, but increases the complexity of the manufacturing process, because an additional mixing step is necessary.
Table 4.5 gives an overview of all the listed silicone, excluding encapsulating resins, in the "Space Material Database" of Dr.Antonius de Rooij, which combines data from different databases like the "European Space Material Database" or the "Materials and Processing Information System" at NASA [18]. The listed properties of pot-life, mixing ratio, max elongation, tensile strength and max-/min temperatures was added from the data sheets of the manufacturer (see source column). All the relevant data sheets can be found in Appendix A.

Table 4.5.: properties of different silicone adhesives source: [18]

name	**manufacturer**	**pot-life** [min]	**mixing ratio**	**max. elongation**	**tensile strength** [$N\,mm^{-2}$]	**min. temp** [°C]	**max. temp.** [°C]	**cost**	**space experience**	**recommended application**	**source**
DC 93-500	Dow Corning	160	10:1	140%	8.5	-65	200	very high	extensive	potting compound for environmental protection of electronic assemblies	[19]
RTV S 691	Wacker	90-110	9.1	100-160%	4.0-6.0	-180	200	very high	extensive	bonding of solar cells to panel	[20]
CV-2500	NuSil	120	10:1	125%	6.9	-120	300	high	high	potting compound for environmental protection of electronic assemblies	[21]
CV-2566	NuSil	180	200:1	150%	6.6	-120	300	high	high	bonding of solar cells to panel	[22]
RTV 566	Momentive	90	1000.1	120%	5.5	-115	260	very high	extensive	bonding of solar cells to panel	[23]

Of all the listed silicone the adhesive "RTV-S 691" from "Wacker", the "CV2566" from "NuSil" and the "RTV566" from "Momentive" are recommended by the manufactures for the use in solar arrays. The mixing ratios of the adhesives "CV2566" and "RTV5662 are extreme. This complicates the precise mixing of the adhesive especially in small quantities. Therefore the adhesive "RTV-S 691" from "Wacker" was selected. It's tensile strength of $4\,\mathrm{N\,mm^{-2}}$ is lower than the other adhesive, but the tensile strength is less relevant like previously stated.
The manufacturer states that the adhesive UV stable and it's components have an unmixed viscosity of 55 000 mPa s and 200 mPa s and a mixed viscosity in between 18 000 mPa s and 26 000 mPa s [20].

4.4.2. Application Process

There are different ways to implement the functions in the final design. Table 4.6 shows the functions and there possible implementations. It also lists the advantages (+) and disadvantages (-) of each design. Some of these implementations are discussed in more detail later in the text.

Table 4.6: different implementation of functions and advantages(+) and disadvantages (-)

function	Implementation 1	Implementation 2	Implementation 3	Implementation 4
Adhesive storage	**Small multi use container on tool** +short transport distance +combinable with volume change +container can be reused -complex tool -bigger tool -cleaning of container after application necessary	**Small single use container on tool** +short transport distance +combinable with volume change +no cleaning necessary -complex tool -bigger tool -container can only be used once	**Large external multi use container** +compact tool +good combinable with pumps -long transport distance -long tubes have to withstand pressure -risk of clogged tubes	
Adhesive mixing	**Mixing tube**	**Mechanical mixing by hand**	**Mechanical mixing tool**	

Continued on next page

Table 4.6: different implementation of functions and advantages(+) and disadvantages (-) (Continued)

	+mixing directly before application +similar adhesive properties every time -difficult in extreme mixing ratios (10:1) -near impossible in large viscosity differences -complex tool	+very simple +no additional tool necessary -additional time -additional out gassing step necessary -limited reputability	+mixing directly before application +similar adhesive properties every time -needs high flow rates -has to be cleaned every time -large size -heavy -expensive	
Adhesive dispensing	**Pneumatically actuated volume change** +relatively small +all components already available -dispensed volume dependent on viscosity -changing process parameters over time when adhesive cures	**Stepper motor and screw drive actuated volume change** +high precision +large traversible distance +volume dispensing independent of viscosity -relatively large -additional end switches necessary	**Linear motor actuated volume change** +high precision +volume dispensing independent of viscosity +smaller than screw drive -short traversible distance -expensive	**Adhesive pump** +could be placed outside of tool -nearly impossible at high adhesive viscosity
Fixation of support panel	**Clamping from the sides** +low profile -possible damage to honeycomb core	**Clamping from the top** -might be in the way of the robot	**Positive lock** +low profile -has to be adjusted to panel form	
Lifting of cells	**Vacuum suction cups** +gentle on cells +vacuum can be externally controlled +pump already available	**Clamping cells from side** +strong grip on cells -might potentially damage cells -actuator on tool necessary		
Rotation of cells	**Using Robot and lifting tool** +no additional tools necessary			
Pressure application	**Internal force sensors of robot** +no additional tools necessary -low precision	**Compression of springs** -force can be precisely controlled -higher complexity		

Continued on next page

Table 4.6: different implementation of functions and advantages(+) and disadvantages (-) (Continued)

Surface cleaning	**Cleaning by hand** +very simple +no additional tool necessary -additional work time -limited reputability			
Primer application	**Application by hand** +very simple +no additional tool necessary -additional work time -limited reputability	**Primer application tool** +less time consuming for worker -additional tool necessary		
Robot control	**Visual programming interface "desk"** +preprogrammed basic tasks +easy to get started -limited to visual interface -limited to preprogrammed tasks -programming is tedious	**C++ control interface** +full control of all robot functions and sensors +highly flexible +can be coded in C++ -hard to get started -no preprogrammed functions (example: no reverse kinematics)		
Applicator control	**Arduino based** +high flexibility +prior experience	**Dedicated stepper controller** +single integrated unit -less flexible		
Emergency stop	**Emergency stop button** +cuts power to all systems stopping them +simple installation			
Robot applicator communication	**24V I/O interface** +designated interface by manufacturer for external devices -data transfer limited -Arduino works with 5 V	**Direct connection to Modbus** +high data transfer rates +some stepper controllers have a integrated Modbus interface -change of control box of the robot -loss of warranty of robot - reprogramming of Modbus necessary		

Continued on next page

Table 4.6: different implementation of functions and advantages(+) and disadvantages (-) (Continued)

Operator Interface	**Laptop** +designed interface by robot manufacturer			
Mechanical connection	**Mechanical tool interface** +already in use			
Electrical connection	**Cable** +inexpensive -might limit robot movement	**Batterie** +allows flexible robot movement -heavy -expensive -has to be recharged		

4.4.2.1. Adhesive Mixing

Before the adhesive is applied both components have to be mixed together so the chemical reaction can start. The selected adhesive "RTV-S 691" must be mixed in a ratio of 9:1 and the components have a viscosity of 55 000 mPa s and 200 mPa s which is a factor of 275:1 between them [20].

Mixing tube A mixing tube is a tool consists of a tube with a mixing coils inside of it. Adhesive is pressed into the tube from the top in two separate streams and this forms a two layer stream which is then separated and stacked on top of each other by a coil. This is repeated until all the layers are so thin that they are indistinguishable. For example a mixing tube with 18 coils has 262144 layers [2]. This System exist as an expensive reusable system in metal form, which has to be cleaned after every application process, and also as a cheap single use system out of plastic, which has to be disposed of after every application process [6]. Picture 4.8 shows such a plastic mixing tube. The advantage of these systems are their simplicity, because no additional movable parts are necessary. Also for the plastic tubes no additional process steps are necessary. This process has problem handling extreme differences in viscosity and is limited to a viscosity ratio of below 100:1. Another important disadvantage is that large mixing ratios can be difficult and mixing ratios above 10:1 are impossible [6].

Mechanical mixing by hand The adhesive can also be mixed by hand with a mixing stick. This process is very simple and suited for the mixing of small batches. The problem with this is, that it takes more time for the worker, because another manual step is required. It also necessitates the removal of air from the adhesive in a vacuum, which is another time consuming step which reduces the available work time with the adhesive, because it has to happen after the mixing and start of the curing reaction. This is necessary, because air gets trapped inside of the adhesive when mixing under a normal atmosphere. This air can reduce the strength of the adhesive and can form bubbles under vacuum which can cause damage to the cells and the rest of the adhesive.

Mechanical mixing tool A mechanical mixing tool consists of a round chamber with a mixer inside turning at a high speed. Both parts of the adhesive are pushed into the chamber via two tubes where they are mixed together by the mixer. The mixed adhesive is pushed out of the chamber by the following adhesives. These systems have the advantage that mixing of two components with vastly different viscosity and extreme mixing ratios is possible. During the nominal mixing process, when the chamber is completely filled by adhesive, no air is mixed into the adhesive. But this is not true for the starting process when air is still present in the chamber. Therefore the first adhesive can not be used and has to be disposed of. another operational disadvantage of this system is, that it has to be cleaned after finishing the application process. Hence this tool is unsuited for the small batch sizes. Further disadvantages are its high weight due to the need of a strong motor for the mixer and its high price [6].

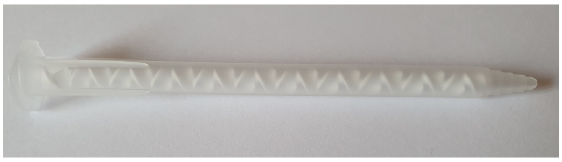

Figure 4.8.: picture mixing tube

In the end the mixing by hand was selected. Because the use of a mixing tube was not possible due to the high difference in viscosity for the selected adhesive. This process can also not be used for the other possible RTV-2 adhesives, because their mixing ratios are larger than 10:1 (see table 4.5). The mechanical mixing tool was also not a good match for this process, because it is not well suited for small batch sizes. This leaves the hand mixing as the only viable option.

4.4.2.2. Adhesive Dispensing

The adhesive has to be moved from its container and dispersed onto the support panel. The flow of the adhesive has to be continuous and should not change in mass flow during the dispensing process. This flow also has to be stopped in between.

Pneumatically actuate volume change In this implementation the volume of the storage container is changed by compressing it with air. For this a small storage container is on the dispensing tool itself. This container has a piston on one side which is pressed by air resulting in a change in volume of the container and an extrusion of adhesive. The actuation mechanism on the tool itself can be very small, because the compressor and valves needed for the operation can be placed outside of it. The big disadvantage is, that the required force for the movement of the piston is related to the viscosity of the adhesive. Hence the necessary force changes during the process time when the adhesive cures, necessitating the pressure to change. This makes the hole process hard to control, because the pressure has to continuously change. This change is influenced by time after the mixing of the adhesive and the temperature.

Stepper and screw drive actuated volume change In this implementation the volume of the storage container is changed by a screw drive powered by a stepper motor. Like in the previous implementation a storage container is placed on the tool itself and a piston is used to reduce the volume of the container and extrude the adhesive. But in this case the piston is connected to a screw drive. When the screw is turned the piston moves linearly up and down the tubes axis. This movement is only dependent on how far the screw has been turned. A stepper motor is a special type of electric motor whose movement can be precisely controlled. This implementation has the advantage that the change in volume is only dependent on the turning of the stepper motor and therefore independent of the viscosity of the adhesive. This implementation has the disadvantage that the hole system is bulky and that at the start the initial position of the piston is not known. This makes it necessary to include an additional switch at the starting point for calibration.

Linear Motor actuate Volume Change This implementation is similar to the one with the stepper motor but uses a linear motor instead. A linear motor directly produces a linear motion. But the distance it can cover is limited. This implementation is simpler than the one with an additional screw drive, but the volume of the container is limited to very small sizes due to the small range of the motor.

Adhesive Pump In this implementation the adhesive is stored in a container outside of the tool and then pumped towards it in a tube. This is the most compact and simple for for the dispensing tool, because it is just a nozzle. But the whole tube has to support the necessary pressure for the pumping of the adhesive. This pressure would be incredibly high due to the high viscosity of the adhesive. This would drastically increase the size and complexity of the tube making it expensive and hard to handle. In addition to that the whole tube has to be cleaned before the adhesive can cure in it or it has to be replaced every time.

The implementation with the stepper motor was selected, because it is independent of the current viscosity of the adhesive making it the easiest to control. Also it is more flexible than the linear motor due to its larger range.

4.4.3. Selected Design Options

The other selected options are described in the following text. For he adhesive storage the small single use container was selected, because it has a good synergy with the selected dispensing method. The positive fit was selected for the fixation of the support structure, because it has a low profile and does not run the risk of damaging the honeycomb. The cells are lifted by vacuum suction cups, because this solution is simpler and does not risk damaging the cells. The application of pressure uses the internal force sensors of the robot, because this decreases the complexity of the handling tool and the robot is already available and precise enough. The primer is applied by hand, because it is the most simple solution, but at the time of writing it is not clear if a primer is even necessary. The robot is controlled with the "DESK" visual programming interface, because the alternative C++ control interface, while being more flexible, comes without a lot of basic functionalities and programming those is beyond the scope of this thesis. The dispensing tool is controlled by an Arduino, because prior experience with this micro controller already existed. The communication uses the 24V I/O Interface, since the other options voids the warranty. A cable is used to power the tool, as it is a simple solution that does not add a lot of weight.

5. Detailed Design

Based on these parameters, requirements and selected implementation a dispensing tool and a handling tool for the "Panda" robot were designed. The CAD-models are created with the software "Solidworks 2019" from "Dassault Systemes". They are designed for rapid prototyping with 3D-printers.

5.1. Dispensing Tool

The dispensing is used for the application of the adhesive. The adhesive is stored in a syringed, that is placed in the tool. The syringe can be compressed by a screw drive to dispense the adhesive. This is done continuously while the robot moves around the tool to place an adhesive pattern on the support structure. Figure 5.1 shows the dispensing tool in use during the adhesive application process.

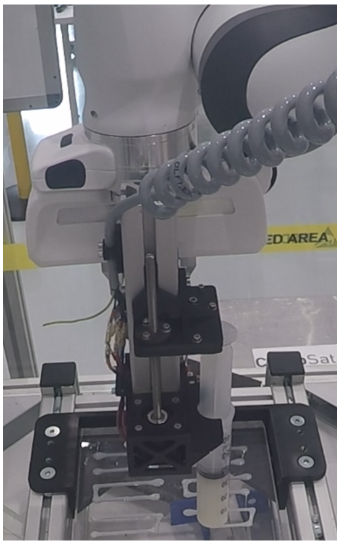

Figure 5.1.: picture of the dispensing tool while working

5.1.1. Mechanical Design

The mechanical structure of the dispensing tool, show in figure 5.2, is based around an "ITEM Profile 8" aluminium extrusion. All the other eleven structural parts are 3D-printed. The adhesive is stored in a syringe and its piston is used to dispense it. They can be removed and disposed of after the bonding process and do not have to be cleaned. The syringe body is connected to the bottom of the aluminium extrusion by a 3D-printed part in which the syringe can be clipped into. The piston of the syringe is placed into a 3D-printed part called the "piston connector", that is connected to the nut on the lead screw of the stepper motor. This part can be moved one axis by the rotation of the motor. This movable part is supported by guide pieces, that run in the groves of the aluminium extrusion and act as a linear bearing that limits the movement of the piston connector to up and down. The stepper motor and the limit switch are also connected to the bottom of the aluminium extrusion by 3D-printed parts.

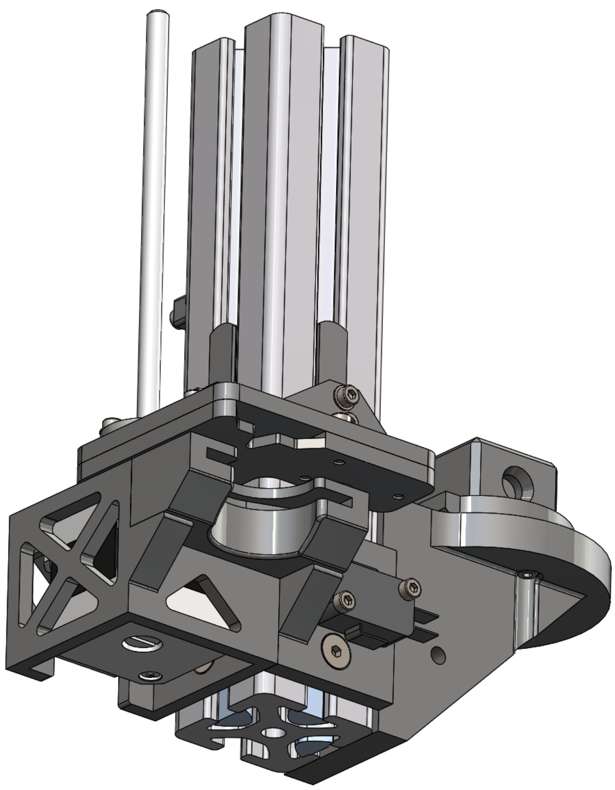

Figure 5.2.: dispensing tool without syringe

On the side not visible in figure 5.2 are additional 3D-printed parts. These act as an release for the connected cable. On the right side of figure 5.2 the mechanical interface for the robot is visible. The robot can grab onto it from above. The robot has to grab the tool from above, because otherwise, due to the limitations in the robot's joints, it wouldn't be able to reach all parts of the solar panel. The mechanical interface is also placed as low as possible to reduce to effective height of the dispensing tool. For a complete bill of materials used in this tool see Appendix C.

5.1.2. Electrical Design

The stepper motor is a "LSA21S14-A-TJCA-152" from "Nanotec". It is a NEMA 17 stepper motor with an integrated lead screw for a linear crew drive. The combination of motor and screw drive can move with up to $55\,\mathrm{mm\,s^{-1}}$ and can provide a maximum force of 250 N, with a resolution of 0.01 mm per step. The lead screw has a length of 152 mm [24]. See Appendix B for more detailed information about the stepper motor. This stepper was selected for its compact design with an integrated lead screw.

The stepper motor on the dispensing tool is controlled by a circuit board below the control cabinet of the robot. The stepper motor and the limit switch are connected this circuit board by a spiral cable. This spiral cable is flexible and allows the robot to move around the dispensing tool. The cable has 7 cores, one of them is for ground, and each core has a cross section area of 0.75 mm.

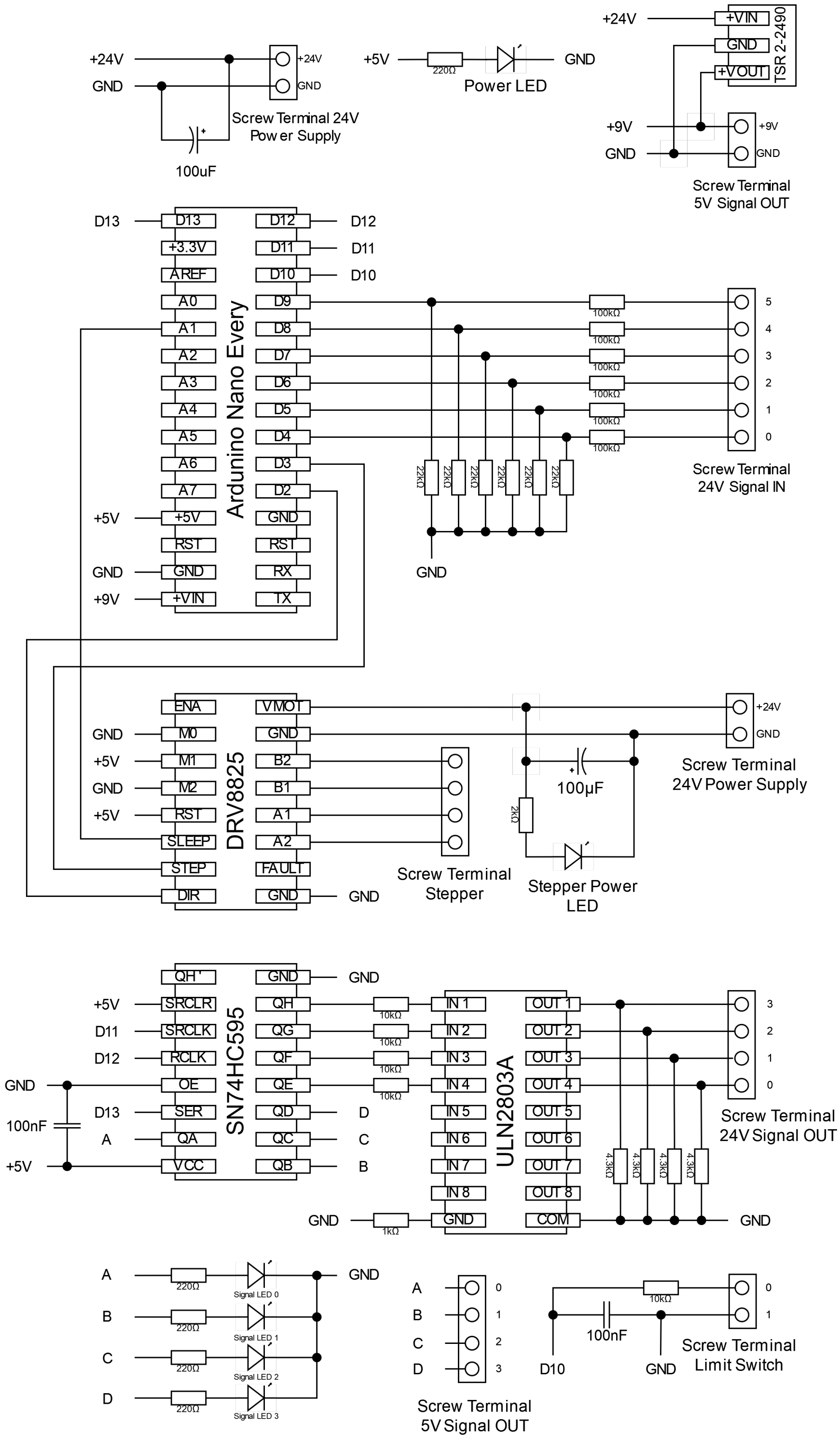

Figure 5.3.: circuit diagram of the dispensing tool

The figure 5.3 shows the circuit diagram of the control board. The heart of this control board is an "Arduino Nano Every" micro controller. The stepper motor is controlled by an "DRV8825" stepper motor driver. This driver limits the maximum current of the stepper motor to 1.4 A, to avoid damaging the motor with too high currents. The driver can move the stepper one step when it gets an control impulse on the STEP pin from the Arduino. The pin DIR controls the direction and the SLEEP pin activates the driver when it is pulled up to 5 V. The pins M0, M1 and M2 are connected in a way, that activates quarter micro steps, which means that every step the motor makes is only a quarter of the size of a regular step. The stepper motor has its own 24 V power supply and a 100 µF capacitor to smooth out any disturbances from the inductive load of the motor.

The rest of the control board is connected to the 24 V power supply of the robot control cabinet, but this power source has not enough power to also drive the motor. This voltage is brought down to 9 V by the "TSA 2-2490" DC/DC converter to power the Arduino by the +VIN pin. The internal power converter of the Arduino is used to provide the 5 V power. At all the power inputs a LED indicates if power is active.

The Arduino gets its commands from the robot controller in form of 24 V signals. To avoid damaging the Arduino the signals are connected to a voltage divider. This lowers the voltage at the Arduino to below a safe 5 V and acts as a pull-down resistor. The use of a simple resistor based voltage divider is possible, because the signal and the power supplied from the control cabinet share the same ground, otherwise the circuits would have to be galvanically isolated from each other. The control board has six 24 V signal inputs.

The Arduino can send back information by four 5 V signal outputs and four 24 V signal outputs. Both outputs are controlled by a "SN74HC595" shift register to reduce the number of pins needed on the Arduino. For the 5 V signal the output of the shift register is directly connected to the output of the board, but they also activate LEDs to give a visual feedback to the operator. For the 24 V signal the 5 V signal of the shift register is turned into a 24 V signal by a "ULN2803A" darlington transistor array. This process also inverts the signal. The limit switch is connected to the pin 10 of the Arduino. It is connected in parallel to a capacitor to limit the filter the interference from the power cables of the stepper motor, because they have to run close to each other in the spiral cable. Annex shows a picture of this control board.

5.2. Cell Handling Tool

The cell handling tool is used for the movement of the cell string. It is cable to lifting up and releasing the cell string. It is also used to apply pressure unto the cell string. The robot can apply a downward force to it, which is transmitted to the cells. Figure 5.4 shows the handling tool while it is used to pick up a string of dummy cells.

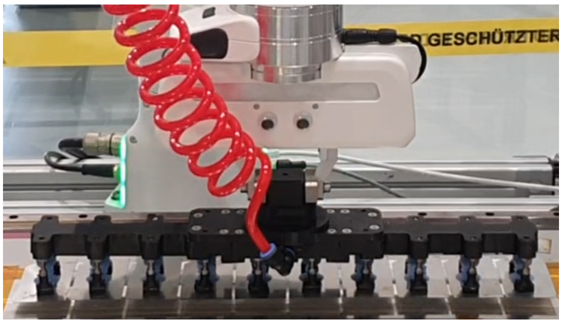

Figure 5.4.: picture of the cell handling tool while it lifts up a dummy string

The cell handling tool shown in figure 5.5 primarily consists of 3D-printed parts. It is made up of a 3D-printed central beam. The robot can directly connect to it by the mechanical tool interface. The vacuum suction cups are directly mounted to the central beam. The beam is hollow to connect the suction cups into one unit. This allows the pulling of a vacuum on all suction cups at the same time. These suction cups can lift up the solar cells, when a vacuum is created inside of them. This pulls the cells against the spacers which are also connected to the central beam by screws. These screws allows the adjustment of the spacers to off-set any irregularities in the flatness of the central beam from the printing process. This is necessary to later apply the contact force evenly to the solar cell-string. The hollow inside of the central beam is connected to a spiral tube, which connects the handling tool to the external low pressure source. These is operated by valve, which in turn are activated by the Programmable Logic Controller (PLC) of the robot. Appendix C contains the bill of materials for this tool.

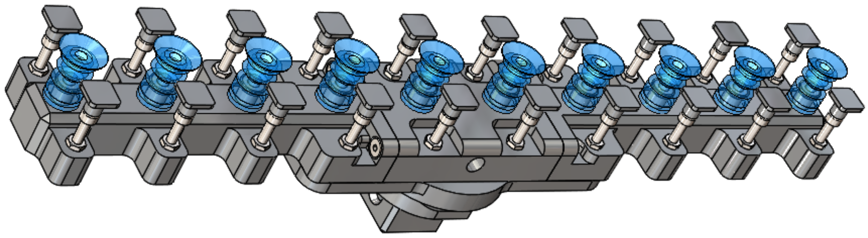

Figure 5.5.: cell handling tool

For the turning of the cell string a 3D-printed comb is added to the side of the production cell. The distances in between the comb are large enough for the suction cups and spacers of the handling tool to pass through. Due to the gaps the solar cell-string can be placed on top of it from the bottom and afterward be picket up from the top. This allows the robot to change the side on which it picks up the cells. The support structure of the solar panel is held in place by a 3D-printed parts that can be adjusted by screws so the form a positive fit around it.

5.3. Software

5.3.1. Robot Control

The robot is controlled with the browser based interface "DESK" from the robot manufacturer "Franka Emika". This is a graphical programming interface, where all the different basic function the robot can perform are blocks called apps. These can be placed after each other to be executed in this order to create more complex tasks.

The movement of the robot can be controlled by three apps. In one them of the robot is controlled by directly changing the angles of the joints. In the other two apps the robot is controlled in Cartesian coordinates. Here the first moves the robot to a position defined in the machine coordinate system, in the other it moves relative to the current end effector position based on changes in the coordinates. The other devices that are connected to the robot can be controlled by switching the 24V signal on the PLC in the control cabinet on and off. This can be done in the program by activating or deactivating modbus signals. In the same way it can be registered what the status on the signal inputs is and the robot can for example wait for a certain signal. For the bonding process multiple different programs were created for the different steps. This includes programs for:

- the changing of the tool
- application of adhesive
- pick-up and turning of the cell-string
- placing of the cell-string on the adhesive

These programs have to be started by the operator, but work automatically afterward. The exact sequences of programs and there operation is described in section 7.2.

5.3.2. Dispensing Tool Control

For the control of the dispensing tool the C based programming language of the Arduino is used. The Arduino micro controller together with the stepper motor driver controls the stepper motor based on the 24 V signals from the PLC of the robot. It is to note that the Arduino only receives a 5 V signal due to the voltage divider in the electronic circuit, otherwise the micro controller could be damaged (see section: 5.1.2). It also sends back 5 V and 24 V Signal to indicate the completion of a task or the occurrence of a problem. in this program the open source library "AccelStepper" by Mike McCauley was used for the control of the stepper motor. This library provides an interface for the control of stepper motor and provides such functions as defining the used acceleration.
The program can perform different tasks based on the 24 V Inputs. Table 5.1 shows the different tasks performed based on which pins are connected to 24 V (HIGH) or connected to GND (LOW).

Table 5.1.: pin configuration for the control of the dispensing tool

pin configuration				**executed task**
Pin0	Pin1	Pin2	Pin3	
LOW	LOW	LOW	LOW	nothing
HIGH	LOW	LOW	LOW	nothing
HIGH	HIGH	LOW	LOW	nothing
LOW	HIGH	LOW	LOW	move to position: low
LOW	LOW	HIGH	LOW	move to position: middle
LOW	HIGH	HIGH	LOW	move to position: high
LOW	LOW	LOW	HIGH	calibration run
HIGH	LOW	HIGH	LOW	move slow: down
HIGH	LOW	LOW	HIGH	move fast: down
HIGH	HIGH	HIGH	LOW	move slow: up
HIGH	HIGH	LOW	HIGH	move fast: up
HIGH	LOW	HIGH	HIGH	move short distance: down
HIGH	HIGH	HIGH	HIGH	move short distance: up

The four main tasks performed by the dispensing tool are the following:

move to position The stepper motor is turned until the piston connector reaches a predefined position. Low is at the bottom of the screw, middle is at half the length of the screw and high is at the top of the screw.

move This turns the screw either fast or slow based on if Pin2 or Pin3 are active. The direction is determined by Pin1. This also checks that the piston connector does not leave its upper and lower boundaries and collide with the calibration switch or falls of on one end. If the boundaries would be violated by any further movement in this direction the task is not executed and the output 0 (lower boundary) or 1 (upper boundary) are set high.

move short distance This task quickly moves the piston connector a short distance up or down. The goal of this is to stop or start the adhesive flow when the application of one pattern is started or finished.

calibration run This task is used for the calibration of the position of the piston connector. First the connector is moved upwards a short distance for the case, that the piston connector already is at the calibration switch. Afterwards is it moved downwards slowly until it activates the calibration switch and its circuit is closed. During this process the lower boundary is ignored and the position of the piston connector is set as the new lower boundary once it hits the switch. Finally the piston connector is moved up a short distance and output 3 is set high for a short time to indicate that the calibration process is finished.

6. Experiments

In this chapter the different experiments are described that were done with the developed system. These experiments should check previously made assumption and help fine tune small parts of the process. For every experiment the setup, execution and observation is described. The observations are analyses and recommendation for the bonding process are derived.

6.1. Extrusion flow experiment

The goal of the experiment is to check the initial assumption, that the mass flow of the adhesive is linear dependent on the speed of the stepper motor. In this experiment an alternative silicon adhesive is used, due to the high cost of the selected adhesive. The silicone used is the A component of the Wacker Elastosil M4642 because this component has a similar viscosity to the mixed Wacker RTV 691.

6.1.1. Setup

Equipment:

- Component A of the silicon test adhesive
- Extrusion tool with stepper motor and screw drive
- Stepper motor controller
- Syringe with piston
- Plastic cups
- Scales
- Vacuum pump

The adhesive is put into a plastic cup and afterwords the air is removed from the adhesive in a vacuum for 30 min. Subsequently it is filled into a syringe and placed in the extrusion tool mechanism. A plastic cup is put underneath to collect the possible spillage. Figure 6.1 shows the set-up.

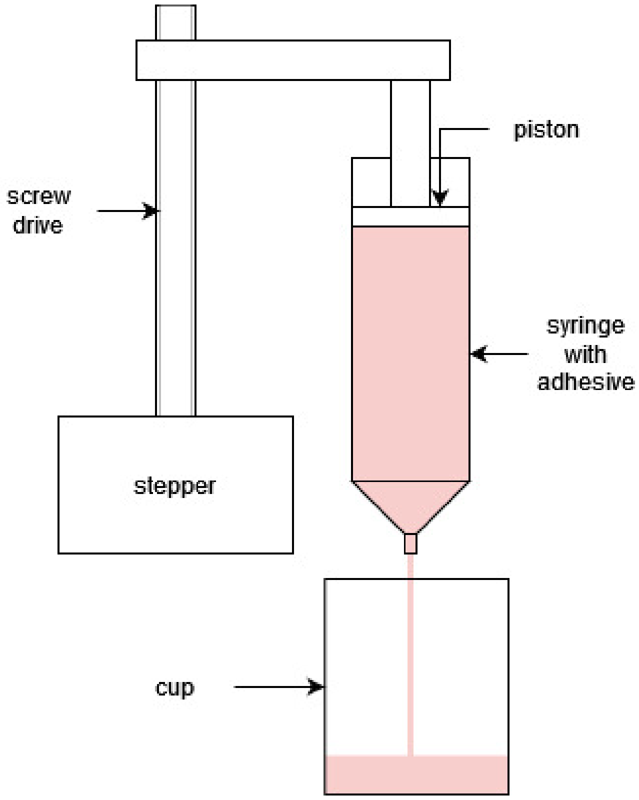

Figure 6.1.: extrusion flow experiment set-up

6.1.2. Execution

The extrusion tool uses a stepper motor and a screw drive to push down the piston of the syringe and force out the adhesive into a collection cup. The rotational speed of the stepper motor can be controlled in steps/s and the screw drive translates this in a linear motion. In this case a stepper speed of 1 steps/s equates to $2.5\,\mu m\,s^{-1}$ of linear speed of the piston. At the start of each round the mass of the collection cup is measured and placed under the syringe. Afterwards the stepper motor is run at different speeds for 60s to extrude the adhesive. After the 60 s the collection cup is removed and weighted. The difference in mass is the adhesive which was extracted in this time. To ensure the exact timing the controller of the robot was used for the control of the stepper motor. Furthermore the adhesive should not change viscosity, because only one component is used and therefore no curing reaction happens.

6.1.3. Observation

Temperature: 20.8 °C

Humidity: 56.0 %rH

For the first speeds the stepper runs smoothly and the adhesive starts flowing when it moves. In between the step speeds 24 steps/s and 27 steps/s the syringe had to be refilled with adhesive. At the stepper speed 30 steps/s the stepper stops running smoothly and starts shaking at the very end of the 60 s extrusion time. At even higher speeds, the shaking increases. Table 6.1 shows the measured data and flow rate, which was calculated by dividing the Δm by 60 s.

Table 6.1.: extrusion flow experiment data

ω_{step} [steps/s]	v_{ext} [µm s^{-1}]	m_0 [g]	m_t [g]	Δm [g]	$\dot{m}$ [mg s^{-1}]	**comment**
3	7,5	2,85	3,51	0,66	10,933	
6	15	3,51	4,48	0,97	16,233	
9	22,5	4,48	5,95	1,47	24,467	
12	30	5,95	8,29	2,35	39,100	
15	37,5	8,29	11,99	3,70	61,583	
18	45	11,99	16,24	4,25	70,783	
21	52,5	16,24	21,38	5,15	85,783	
24	60	21,38	27,41	6,03	100,433	
27	67,5	2,83	10,01	7,18	119,583	refill cup change
30	75	10,01	18,27	8,26	137,633	starts shaking at the end
33	82,5	18,27	28,91	10,65	177,450	some shaking
36	90	28,91	40,46	11,54	192,367	some shaking
39	97,5	40,46	51,99	11,54	192,250	some shaking
42	105	51,99	61,72	9,73	162,133	a lot of shaking back and forth

6.1.4. Analysis

In the beginning the flow rate is slowly increasing, this might be due to the fact, that some air might be left in the syringe, which first has to be compressed, or that the extrusion tool first deforms a little, because it is not very stiff due to the fact that large parts are made of 3D-printed plastic.
The area in the middle follows a line. Therefore, the points from 22.5 mm s^{-1} up to 75 mm s^{-1} can be approximately described by a linear equation. Using the least squares linear regression following function can be found (see the orange line in figure 6.2):

$$\dot{m} = 2.104\,96\,\mathrm{mg\,\mu m^{-1}} * v - 22.6963\,\mathrm{mg\,s^{-1}} \tag{6.1}$$

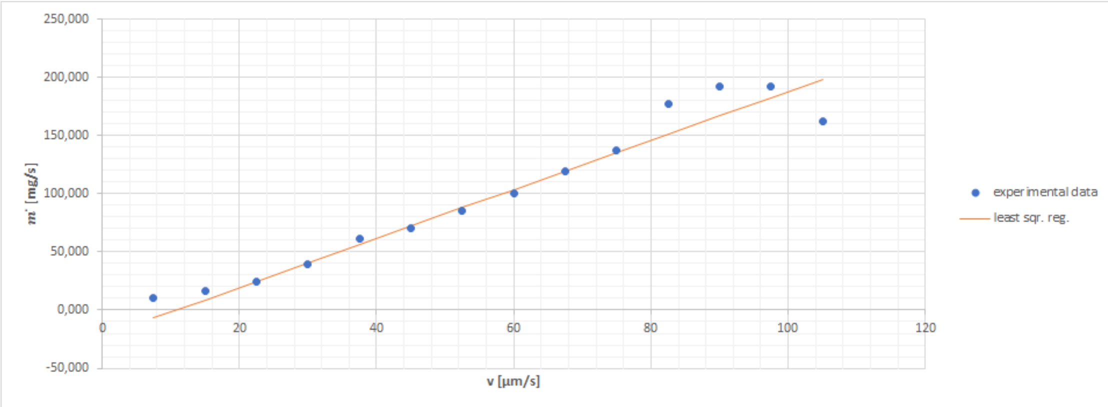

Figure 6.2.: extrusion flow experiment data with linear regression

The shaking at the end indicates that the stepper is skipping steps. This can happen if the torque for moving to the next step is greater than the maximum torque of the stepper. This indicates, that the force needed to extrude the adhesive at this speed is greater than the force the stepper with the screw drive can provide. But this does not explain the increase in the mass flow of the adhesive in this area. If the stepper is skipping steps this should reduce the effective speed of the stepper and therefore should reduce the mass flow. An explanation for this observation might be, that the additional vibration of the stepper increases the mass flow rate. This might be the case, because the flow rate of non-Newtonian fluids like the adhesive can be increased by vibration [25].

6.1.5. Conclusion

The initial assumption of a linear relationship between the extrusion speed and the mass flow is correct for the speed range of $22.5\,\mu m\,s^{-1}$ to $75\,\mu m\,s^{-1}$. Therefore the used speed should be in this range, but an additional margin should be subtracted from the upper limit, because the viscosity of the curing adhesive will increase in time and subsequently the stepper should start skipping earlier. The early build up phase can be crossed quickly by selecting a high acceleration rate and the later overloading range should be avoided.

6.2. Line width experiment

The goal of the experiment is to determine what influence the movement speed of the robot has on the line width. It would be expected, that an increase in the movement speed of the robot would reduce the amount of adhesive per length and therefore decrease the line width. In this experiment an alternative silicon adhesive Wacker Elastosil M4642 is used, due to the high cost of the selected adhesive (see section 6.1).

6.2.1. Setup

Equipment:

- Component A of the silicon test adhesive
- Extrusion tool with stepper motor and screw drive
- Stepper motor controller
- Syringe with piston
- Plastic cup
- Franka Emika Panda robot
- Plexiglas plate
- 10 dummy cells
- Vacuum pump
- Tape
- Cell-handling tool

The adhesive is put into a plastic cup and afterwards subjected to a vacuum for 30 min to remove the air from it. Subsequently it is filled into a syringe and is placed in the extrusion tool mechanism. The Plexiglas plate is cleaned and placed in the position for the back-panel. Also a string of cells is created by taping multiple cells together, for this it is important to tape them together on the top side, so the tape does not come in contact with the adhesive, because this might influence the results.

6.2.2. Execution

First some of the adhesive is extruded from the syringe using the extrusion tool to remove any impurities and to get a consistent flow. After this the robot uses the extrusion tool to create two lines of adhesive with a length of 60 mm and a distance of 20 mm to each other at the place of one cell on the Plexiglas plate. This is repeated for all the cells at different speeds for a total of 10 cells. The speed in the desk programming interface is varied by a factor of 1% of the maximum speed with results in a speed of $15\,\mathrm{mm\,s^{-1}}$ per %. After this the tool is changed from the extrusion tool to the cell-handling tool. The tool is then used to place the string on top of the adhesive and is moved toward the plate until a force of 20 N is reached. Afterwords the handling tool releases the string and is moved away. Following this the string is fixed in place with tape to prevent it from moving around. This is necessary, because the single component of the adhesive does not cure. Finally the Plexiglas is turned around and the width of each line is measured and marked. Figure 6.3 depicts how these lines locked and what distance was measured.

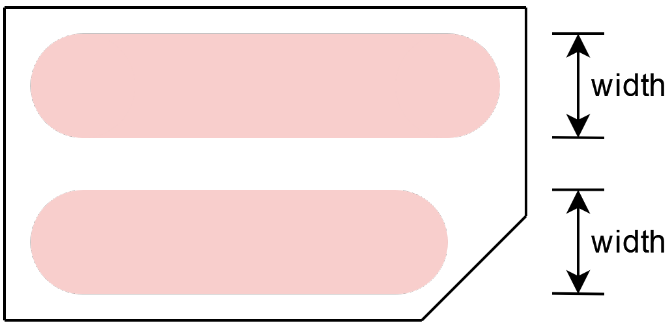

Figure 6.3.: schematic of the placed lines in the experiment

6.2.3. Observation

Temperature: 20.9 °C

Humidity: 55.6 %rH

The resulting lines vary greatly in width. Especially the start and end point of each line is a lot thicker than the rest. The line in between is consistent in size for the slower speeds but varies for the faster speeds. Also the first line is a lot thinner than the second line. Table 6.2 shows the measured width of the lines. If the line was inconsistent the medium width is stated.

Table 6.2.: line width experiment data

Test No.	v_{bot} [%]	v_{bot} [mm s^{-1}]	**Width 1** [mm]	**Width 2** [mm]]	**comment**
1	10	150	3	8	
2	9	135	4	8	
3	8	120	4	9	
4	7	105	4	10	very inconsistent line 2 (7mm to 13mm)
5	6	90	5	7	very inconsistent line 2 (4mm to 10mm)
6	5	75	5	12	
7	4	60	7	14	
8	3	45	5	14	
9	2	30	4	14	
10	1	15	5	19	

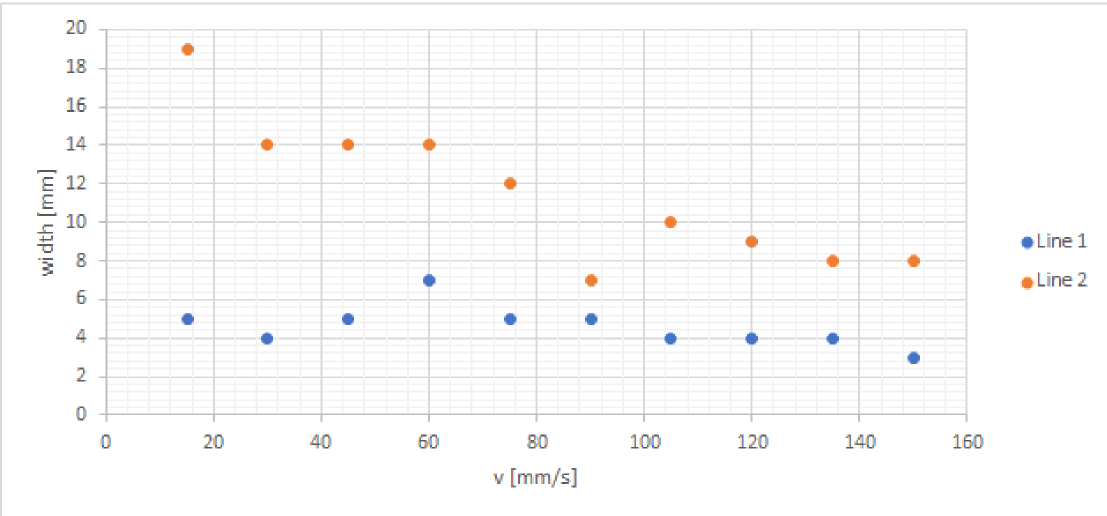

Figure 6.4.: width experiment data)

6.2.4. Analysis

Figure 6.4 shows that for line 2 an increase in movement speed of the robot decreases the width of the adhesive line. This is in accordance with the assumption, that a higher speed decreases the amount of adhesive per length and therefore reduces the width after the addition of the cell. But it also shows that the line width is unstable for faster speeds. This might be due to the fact, that at a slower movement velocities small changes in the

flow rate of the adhesive can be balanced out.
But Line 1 does not show the relationship between movement velocity and line width. This might be caused by the overlap of the cells. At the edge closer to line 1 the connection strips of the previous cell lie under this cell. This increases the gap between the Plexiglas plate and the cell. This indicates, that the line width is more dependent on the contact pressure and gap height than the amount of adhesive (see Figure 6.5). For the real cells it can be expected, that this effect is smaller, because the dummy cells have a height of 0.25 mm and the connectors on the real cells have a height of 0.1 mm.

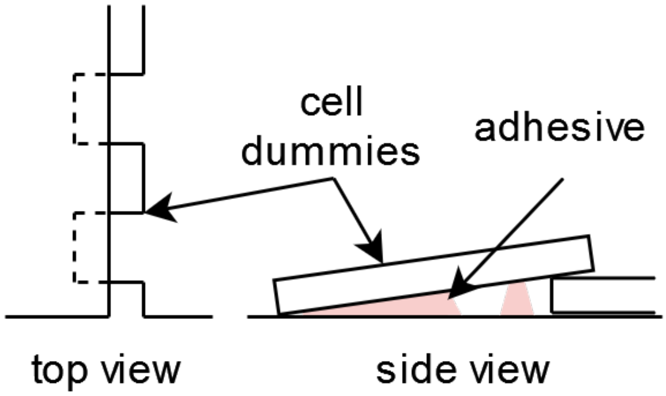

Figure 6.5.: width experiment cell overlap (not to scale)

6.2.5. Conclusion

This experiment showed, that while the width of the adhesive line is dependent on the movement speed of the robot it seams to be stronger dependent on the contact pressure and gap height. It also showed, that the movement speed should not be to high to balance out small changes in the flow rate. Therefore a speed not faster than $75\,\mathrm{mm\,s^{-1}}$ is recommended, while a lower speed might be even better, but this is a trade-off between consistency and manufacturing time.

6.3. Pattern experiment No.1

The goal of this experiment is to compare different adhesive application patterns and evaluate which best fits the requirements from and which is the fastest. The different tested application patterns all can be seen in figure 6.6. The created patterns are open on at least one side to avoid the trapping of air. For this experiment like the ones before the adhesive Wacker Elastosil M 4642 was used as an alternative.

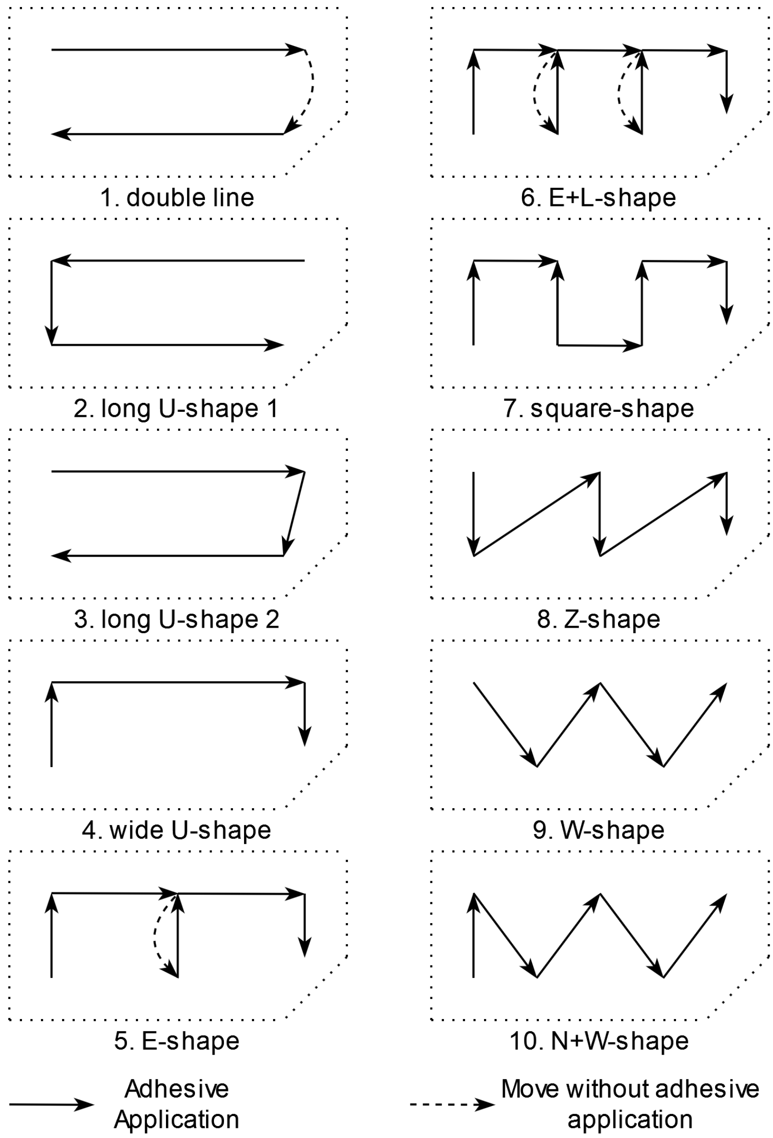

Figure 6.6.: pattern experiment adhesive application patterns

6.3.1. Setup

Equipment:

- Component A of the silicon test adhesive
- Extrusion tool with stepper motor and screw drive

- Stepper motor controller
- Syringe with piston
- Plastic cup
- Franka Emika Panda robot
- Plexiglas plate
- 10 dummy cells
- Vacuum pump
- Tape
- Cell-handling tool
- Timer

The adhesive is put into a plastic cup and afterwards subjected to a vacuum for 30 min to remove the air from it. Subsequently it is filled into a syringe and is placed in the extrusion tool mechanism. The Plexiglas plate is cleaned and placed in the position for the back-panel. Also a string of cells, this time without the overlapping connection strips, is created by taping multiple cells together, for this it is important to tape them together on the top side, so the tape does not come in contact with the adhesive, because this might influence the results. The time, which was build from an Arduino, measured the time between pulses from the PLC of the Robot.

6.3.2. Execution

First some of the adhesive is extruded from the syringe using the extrusion tool to remove any impurities and to get a consistent flow. After this the robot uses the extrusion tool with an extrusion speed of $30\,\mu\text{m}\,\text{s}^{-1}$ and a movement speed of $75\,\text{mm}\,\text{s}^{-1}$ to apply adhesive to the Plexiglas plate. These speeds are selected, because the extrusion speeds is at the lower end of the usable interval (see 6.1) and this gives a margin for error if the viscosity increases. The movement speed is selected, because it is the fastest usable speed (see 6.2). The adhesive is extruded at the place of the first cell of both strings and uses the first adhesive pattern from figure 6.6. This process is repeated for all the other patterns in figure 6.6. Every time the robot starts and stops the application process a signal is sent to the timer, which measures the application time for each cell. After this the tool is changed from the extrusion tool to the cell-handling tool. The tool is then used to place the strings on top of the adhesive and is moved toward the plate until a force of 20 N is reached. Afterwords the handling tool releases the string and is moved away. Following this the string is fixed in place with tape to prevent it from moving around. This is necessary, because the single component of the adhesive does not cure.Subsequently the Plexiglas plate is turned and on the underside trapped air is marked and large distances to the edge of the cell are measured. After this the underside is photographed. This is then repeated after 1 h.

6.3.3. Observation

Temperature: 20.4 °C

Humidity: 53.3 %rH

Table 6.3 shows the time needed for the adhesive application for each cell as well as the average for each pattern type. Figure 6.7 also shows the average time for each pattern.

Table 6.3.: pattern experiment application times

No.	**shape name**	t_1 [s]	t_2 [s]	t_M [s]
1	2x Line	18.14	18.34	18.24
2	long U1	14.69	14.54	14.615
3	long U2	14.66	14.57	14.615
4	wide U	11.81	11.87	11.84
5	E	19.33	19.65	19.49
6	E+L	27.17	26.97	27.07
7	square	16.41	16.36	16.385
8	Z	15.44	15.03	15.235
9	W	13.12	13.02	13.07
10	W+N	14.85	14.97	14.91

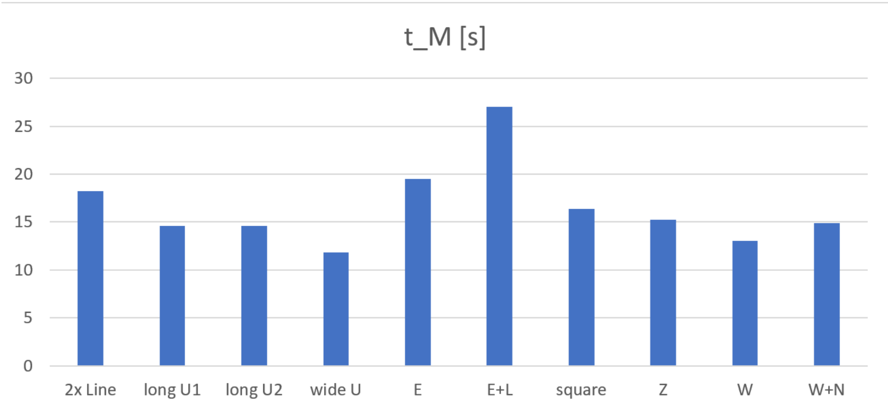

Figure 6.7.: pattern experiment average times for the application of each pattern

Directly after the placement of the cell string the patterns No.1-3 have trapped air inside the adhesive. In the pattern No.4 the distances between the adhesive and the edge of the cell are large with 23 mm and 22 mm. A similar result can be seen in pattern No.9, with distances to the edge of 22 mm and 20 mm. This can be seen in Figure 6.8, which shows a picture taken directly after the placement of the cells.

Figure 6.8.: pattern experiment plate underside directly after cell placement (No.1 to No.10 is right to left)

After 1 h the adhesive is more spread out and it has closed the gaps, which trapped small air bubbles in the patterns No.6 and No.7. Air is also still trapped in the patterns No.1-3. The distance to the edge was reduced in almost all patterns but in pattern No.4 it is still

19 mm to 20 mm and in pattern No.9 it is 16 mm to 20 mm. The next largest distance to an edge is pattern No.8 with 8 mm. In most patterns some adhesive is pushed out from under the cells. Figure 6.9 shows a picture taken of the plate's underside after 1 h with additional markings to highlight the trapped air and the distance to the edge.

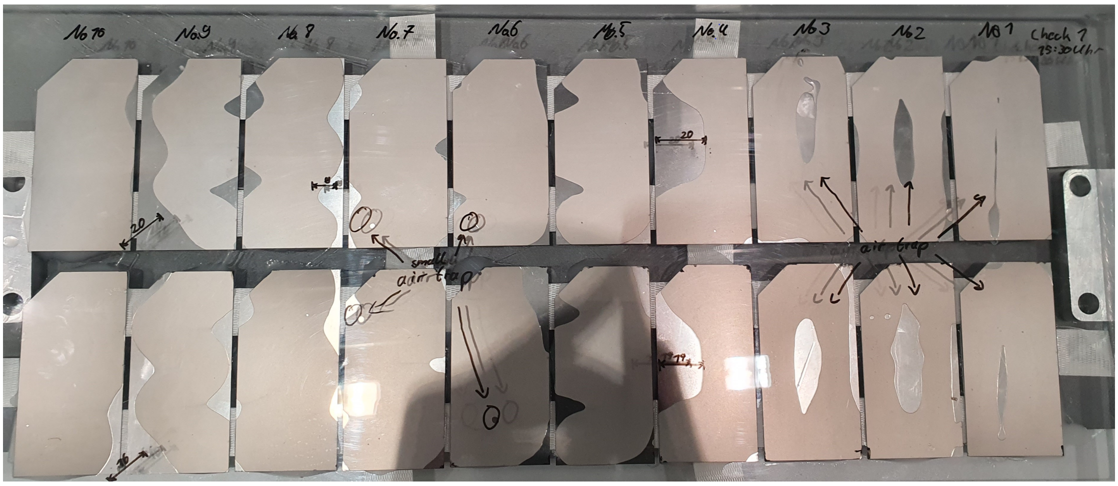

Figure 6.9.: pattern experiment plate underside with markings after 1 hour

6.3.4. Analysis

The time each pattern takes is influenced by the length of each application line but more by the amount of interruptions of the extrusion. The pattern No.1,5,6 are longer than all the other patterns. Especially pattern No.6 with two stops is with an average time of 27.07 s longer than pattern No.7 with an average time of 16.39 s despite both having the same application path length. This is caused by the fact, that every time the extrusion is stopped the piston has to be pulled back to stop the flow of adhesive and then has to be moved forward when it starts again. This loses time especially if this has to happen more than once.

If the gap between the adhesive lines is to small air can get trapped in the pattern even if the application pattern is open on one side. This does not seem to happen if the adhesive lines meet in a narrow angle. In this case the gap starts closing at the narrowest point and pushes the air outward.

The adhesive that is pushed out from under the cells is an indication that the used amount of adhesive is to large and that the extrusion speed can be reduced. Of all the tested patterns only the pattern No.8-10 fulfill all the requirements from section 4.3.1. They do not trap air and every point on the cell is close to the adhesive.

6.3.5. Conclusion

From the observations of this experiment it can be concluded, that the final pattern should be continuous to not lose time. Additionally the adhesives lines should meet in narrow angles to avoid trapping air. The pattern No.8 is the most promising pattern for future use, because it is the fastest of the patterns which fulfill the requirements.

But the informative value of this experiment for the behavior off the adhesive after the extrusion is limited, because the used alternative adhesive does not cure and therefore does not stop flowing, while the real adhesive increases in viscosity during the curing process. Therefore this experiment should be repeated with the real adhesive.

6.4. Pattern experiment No.2

This is a repeat of the previous pattern experiment, but with a different adhesive. The adhesive for the real solar panel the Wacker RTV 691 was not available in time for this thesis. Therefore this test was done with the mixed silicone adhesive Wacker Elastosil M4642, but the viscosity of this mixed adhesive is only half of the real adhesive. The goal of this experiment was to evaluate the difference in behavior of the mixed and therefore curing adhesive and the not reacting single component. Another property that was checked is the thickness of the adhesive layer and if it is above 0.1 mm.

6.4.1. Setup

The set-up for this is the same as in the previous experiment with the exception that in addition to the component A also the component B of the Wacker M4642 is needed and that both are mixed in the plastic cup in a ratio of 10:1 prior to placement in the vacuum chamber. Another small change is, that in this experiment the time for each pattern is not measured, because the times for each pattern should not change from the previous experiment. For this reason no timer is connected to the PLC.

6.4.2. Execution and Observation

This test was performed in the same way as the previous experiment, with the exception that pattern E+L shape was removed and the square shape is now pattern No.6 and the Z-shape is now pattern No.7. Pattern No.8 is new pattern shown in figure 6.10.

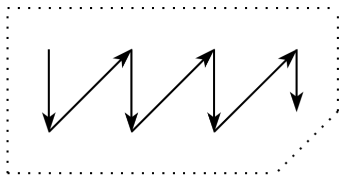

Figure 6.10.: pattern experiment No.2 new dense Z-pattern

It is a new pattern based on the Z-shape, but more dense. In addition the plate with the cells and adhesive was checked after 36 h and the thickness of the cells, plate and adhesive were measured with a caliper.

Temperature: 20.7 °C

Humidity: 54.6 %rH

During the extrusion of the adhesive, the adhesive flow did not always stop, when the piston was pulled back, like in the previous experiment. This caused some additional thin adhesive lines. The adhesive lines directly after the cell placement look similar to the ones from the previous experiment, directly after the placement of the cells. The big different was, that the adhesive did not spread out as much over time. Even after the adhesive was fully cured 36 h later it had not spread much beyond its position directly after cell placement. Figure 6.11 shows a picture taken from the underside after 36 h.

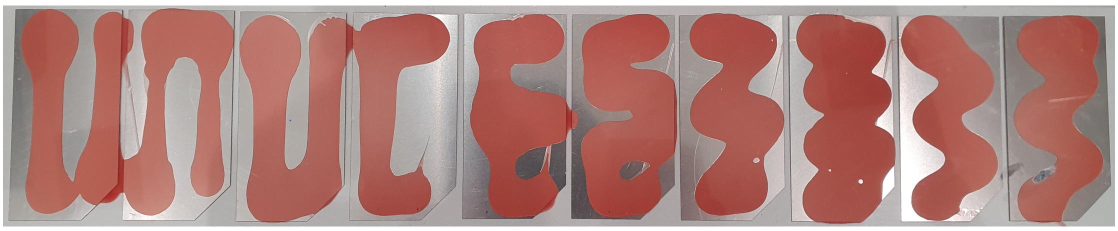

Figure 6.11.: pattern experiment No.2 plate underside after 36 hours

Larger air pockets only got trapped in the E-shaped and square shaped patterns. Also the Z-shape and the new shape have small air bubbles. No separation of cell, adhesive or plate could be observed. Table 6.4 shows the measured thickness of the plate together with the cells and adhesive. The plate on its own has a thickness of 19.6 mm and the cells have a thickness of 0.24 mm. The adhesive layer thickness was calculated by subtracting the thickness of the cells and the plate.

Table 6.4.: measured adhesive layer thickness

No.	shape-name	**total thickness** [mm]	**adhesive layer thickness** [mm]
1	2x Line	20.12	0.28
2	long-U1	20.15	0.31
3	long U2	20.08	0.24
4	wide U	20.17	0.33
5	E	20.20	0.36
6	square	20.30	0.46
7	Z	20.32	0.48
8	dense Z	20.28	0.44
9	W	20.27	0.43
10	W+N	20.29	0.45

6.4.3. Analysis

The initial behavior of the mixed adhesive was similar to the one used in previous test, with the exception, that the adhesive flow sometimes did not stop in time. This might be caused by the lower viscosity compared to the previously used single component. The big difference is the behavior of the adhesive over time. This adhesive did not spread as far as the previous one. This might be caused by the curing reaction, that increases the viscosity of the adhesive or that the adhesive sticks better to the cells and plate. The layer thickness of the adhesive was constantly above the required 0.1 mm. But there the difference between the thickest and thinnest layer were 0.2 mm. This might be due to the fact that in the later patterns with the larger layer thickness more adhesive was used. Another cause for this might be, that the force was not applied evenly by the robot and tool and that one side experienced a larger force.

6.4.4. Conclusion

This experiments shows, that the behavior of the adhesive can differ between different adhesives, which highlights the need for a repeat of this experiment with the adhesive Wacker RTV 691 when it is available. It also shows that the adhesive layer thickness is not constant. This problem might be smaller if the same pattern is used for the whole string. Which is also something that has to be checked with the real adhesive. This experiment also shows that the tools performance was the same despite using a different adhesive. Indicating that only small parameters have to be tweaked for the real adhesive. The good adhesion between cells and plate without use of a primer indicates that the use of one might not be necessary. This has to be verified with the final adhesive and the final support structure, when they are available.

7. Process Overview

This chapter describes the developed robot assisted manufacturing process for solar panels. It gives a short overview of the welding process developed by Patric Seefeld, Sebastian Kottmeier and Toni Devolski. It describes the bonding process developed in this thesis and shows how both processes work together. See also patent [26]. Figure 7.1 show the flow chart of the hole process. It is also shown which tasks are done by a human operator and which tasks are performed by the robot.

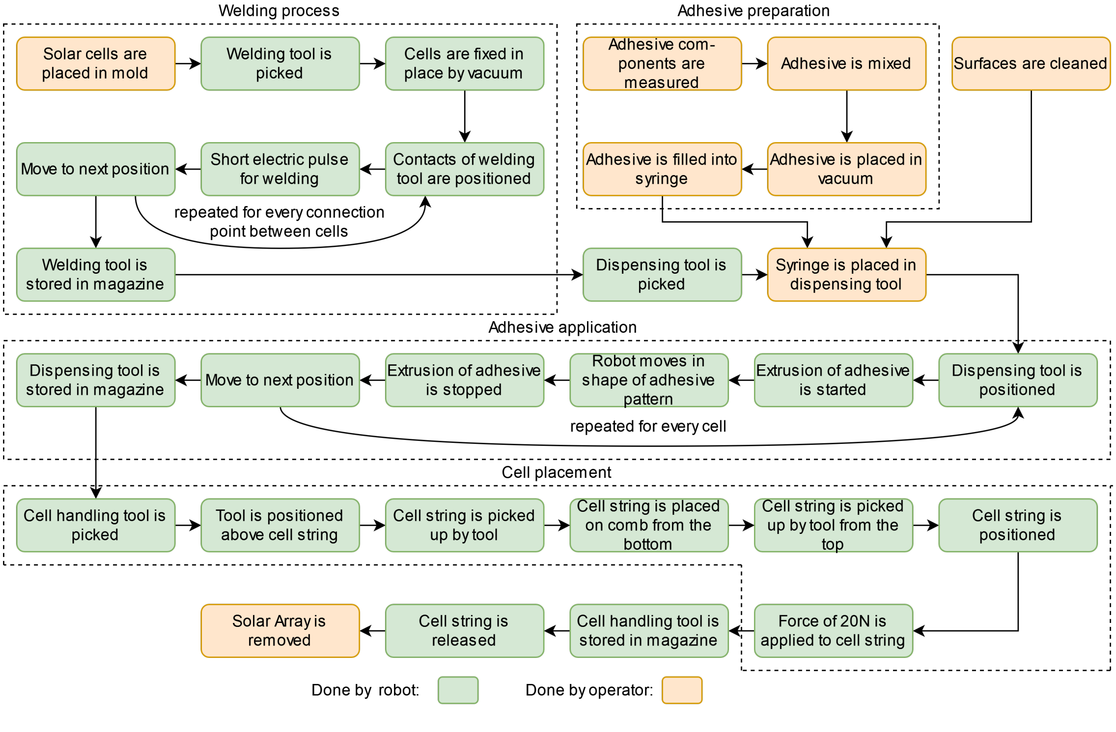

Figure 7.1.: flowchart of the hole process

7.1. Welding Process

The goal of the welding process is to electrically connect the single solar cells together to form a string. To achieve this a spot welding process is used to connect the connection strips of one cell to the backside of the neighboring cell. This uses a tool depicted in figure 7.2.

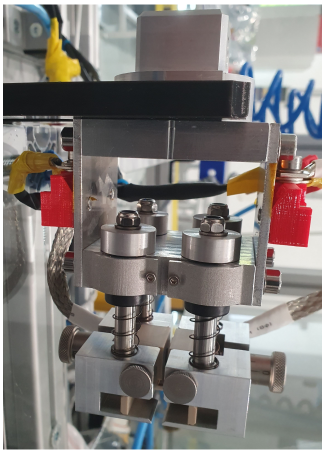

Figure 7.2.: picture of the welding tool

The tool has to electrodes for welding and springs that can regulate the contact force. In this process the solar cells are first placed upside down in a metal mold, so the cells are all spaced evenly with a 2 mm gap in between them. To prevent the cells from moving, they are sucked down with an vacuum. After this the robot places the two electrodes of the welding tool on top of each connection and they are welded together by a short electric pulse. This process takes roughly 1 min for a ten cell string. This results in an average time of 6 s for each solar cell.

7.2. Bonding Process

The bonding process developed in this thesis connects the welded strings from the previous process to the supporting composite panel. In a first step the panel is cleaned with Isopropyl alcohol and a primer is added with a brush to it, if necessary. Afterward the adhesive is prepared. The component are weighted and mixed together. Afterwards the air is removed from the mixture under vacuum. This is done until no new air bubbles rise up from the adhesive. This takes on average 10 min. The mixture is filled into the syringe afterwards.
In the next step different programs are executed on the robot. In the first program the

robot picks up the dispensing tool from the magazine, calibrates the position of the stepper motor and moves the tool in a waiting position for the adhesive. Before the execution of the next program the syringe with the adhesive is added to the dispensing tool. In the next program the robot moves to different point above the support panel in a rectangular grid pattern. Each of these points correspond es to the top left corner of the solar cell, the one opposite the one with the cut out. At each of this points the robot moves downward and the piston of the syringe is moved forward to start the extrusion of adhesive. Afterwards the robot executes a series of relative movements at a speed of $60\,\mathrm{mm\,s^{-1}}$ corresponding to the shape of the selected adhesive pattern. During this time the piston of the syringe is moved forward with a speed of $30\,\mathrm{\mu m\,s^{-1}}$ to ensure a continuous adhesive flow. Afterwards the piston is pulled back to stop the adhesive flow and the robot moves upwards. This is then repeated for all the points. This process should place the same adhesive pattern at the final position of each solar cell. Afterwards the robot puts the dispensing tool back into the tool magazine.

For the final step the tool is changed to the handling tool. With this tool the robot picks up the cell string using the suction cups and an vacuum generated by the compressor. The string together with the handling tool is turned up side down and the string is paced on the comb, with the handling tool below it. The string is released from the tool and picked up again, this time from the top side. This results in the string being held from the other side. This string is positioned on top of the panel and the robot moves down until a collision with the support panel is detected. Now the robot applies a force of 20 N downward onto the string. Afterwards the string is released and the tool is stored back in the magazine.

The preparation of the adhesive together with the filling of the syringe takes an average of 12 min, but up to 60 mL of adhesive can fit into the syringe and can therefore be prepared in one batch. This is enough adhesive for 12 strings of 10 solar cells each, which results in a preparation time of 6 s for each cell. The application of the adhesive takes 16.5 s per cell if the Z-shaped pattern is used. The turning and placement of the string takes again 1 min, resulting in another time of 6 s per cells. Together with the welding process this results in a time of 34.5 s for the welding and bonding of each cell. Each cell can produce up to 1.21 W of peak power. This results in a time of 28.5 s needed for the welding and bonding of one watt of solar panel power. This excludes the time needed for the additional electrical connections and the testing of the cells. But it also does not consider the parallel execution of multiple task, for example the strings can be welded together by the robot, while the operator prepares the adhesive.

8. Conclusion and Outlook

The adhesive bond developed in this thesis theoretically fulfils the requirements and should securely connect the cells to the support structure in all expected situations.However, this could not be verified. Therefore further tests are necessary once the adhesive RTV 691 and a real prototype for the support structure become available. They should be used to manufacture a prototype, which can be used for thermal vacuum chamber and shaker tests. These test should simulate the environment during operation and launch to verify that the adhesive bond does not fail under these conditions.

The designed bonding process should be able to produce the specified adhesive bond. The experiments and test in this thesis show, that the developed tools and processes work. But it could not be tested with the RTV 691. Hence additional test are necessary when the adhesive becomes available. It can be expected, that the processes and tools do not have to be changed, but it can be the case, that small parameters like the extrusion speed have to be adjusted.

Another conclusion from this thesis is, that collaborative robots together with the rapid development of 3D-printed tools can be successfully used in the integration of spacecrafts. This demonstrates that this type of robot can be used in situation previously unsuited for traditional industrial robots. Therefore it should be investigated which other processes in the integration of spacecraft can be improved by the collaboration with robots.

Bibliography

[1] C. D. Brown, *Elements of Spacecraft Design*, 1st ed. Reston: American Institute of Aeronautics & Astronautics, 2002, ISBN: 978-1-600-86051-5.

[2] G. Habenicht, *Kleben* (VDI-Buch), 6th ed. Berlin: Springer, 2009, ISBN: 978-3-540-85264-3.

[3] Papež N., Dallaev R., Ţălu Ş. and Kaštyl J., "Overview of the current state of gallium arsenide-based solar cells," *Materials*, vol. 14, no. 11, p. 3075, Jun. 2021. DOI: 10.3390/ma14113075.

[4] R. Müller, J. Franke, D. Henrich, B. Kuhlenkötter, A. Raatz, and A. Verl, *Handbuch Mensch-Roboter-Kollaboration*, 1st ed. München: Hanser Verlag, 2019, ISBN: 978-3-446-45016-5.

[5] Lucas F. M. da Silva, Andreas Öchsner, Robert D. Adams, *Handbook of Adhesion Technology*, 1st ed. Berlin, Heidelberg: Springer, Jun. 2011, ISBN: 978-3-642-01168-9.

[6] M. Rasche, *Handbuch Klebtechnik*, 1st ed. München: Hanser Verlag, 2012, ISBN: 978-3-446-43198-0.

[7] B. A. Banks and R. Demko, "Atomic oxygen protection of materials in low earth orbit," NASA, Tech. Rep. TM—2002-211360, Feb. 2002.

[8] Franka Emika GmbH, *Panda's Instruction Handbock*. Munich, Apr. 2020.

[9] AZUR SPACE Solar Power GmbH, *30% triple junction gaas solar cell assembly*, https://www.azurspace.com/images/products/0003805-01-01_DB_3G30A.pdf, Aug. 2016.

[10] Space X, *Falcon users's guide*, https://www.spacex.com/media/falcon-users-guide-2021-09.pdf, Sep. 2021.

[11] J. Li, S. Yan, and R. Cai, "Thermal analysis of composite solar array subjected to space heat flux," *Aerospace Science and Technology*, vol. 27, pp. 84–94, Jun. 2013. DOI: 10.1016/j.ast.2012.06.010.

[12] T. Soma, J. Satoh, and H. Matsuo, "Thermal expansion coefficient of gaas and inp," *Solid State Communications*, vol. 42, pp. 889–892, Jun. 1982. DOI: 10.1016/0038-1098(82)90233-2.

[13] R. I. Cottam and G. A. Saunders, "The elastic constants of gaas from 2 k to 320 k," *Journal of Physics C: Solid State Physics*, vol. 6, no. 13, pp. 2105–2118, Jul. 1973. DOI: 10.1088/0022-3719/6/13/011.

[14] P. Hidnert, "Thermal expansion of five selected optical glasses," *Journal of Research of the National Bureau of Standards*, vol. 52, no. 6, pp. 2507–2508, Jun. 1954.

[15] J. Matsuda, "Studies on the young's modulus of silicate glass as a function of temperature," *The Review of Physical Chemistry of Japan*, vol. 30, pp. 9–24, Aug. 1960. DOI: 10.1016/j.ast.2012.06.010.

[16] L. N. McCartney and A. Kelly, "Effective thermal and elastic properties of $[+\theta/-\theta]_s$ laminates," *Composites Science and Technology*, vol. 67, no. 3-4, pp. 646–661, Mar. 2007. DOI: 10.1016/j.compscitech.2006.05.006.

[17] AZoM.com. "Silicone rubber." Accessed: 21.05.2023. (2001), [Online]. Available: https://www.azom.com/article.aspx?ArticleID=920.

[18] D. A. de Rooji. "Space materials database." Accessed: 30.01.2023. (), [Online]. Available: https://www.spacematdb.com/.

[19] Dow Chemical Company, *Technical data sheet: Dowsil 93-500 thixotropic*, https://www.dow.com/en-us/document-viewer.html?docPath=/content/dam/dcc/documents/en-us/productdatasheet/11/11-15/11-1586-dowsil-93-500-thixotropic.pdf, 2017.

[20] Wacker Chemie AG, *Wacker rtv-s 691 a/b*, https://www.wacker.com/h/en-us/medias/WACKER-RTV-S-691-AB-en-2023.04.12.pdf, 2023.

[21] Avantor Inc., *Cv-2500 controlled volatility silicone elastomer*, https://www.avantorsciences.com/assetsvc/asset/en_US/id/29017429/contents/en_us_tds_nusicv-2500.pdf, 2021.

[22] Avantor Inc., *Cv-2566 controlled volatility rtv silicone adhesive*, https://www.avantorsciences.com/assetsvc/asset/en_US/id/29017450/contents/en_us_tds_nusicv-2566.pdf, 2021.

[23] Momentive Performance Materials Inc., *Technical data sheet rtv566*, https://www.momentive.com/en-us/products/tds/rtv566?productid=d69e3b32-66e5-45c0-8e9c-9c2781aabe55, May 2021.

[24] Nanotec Electronic GmbH & Co. KG, *Linear actuator lsa421s14-a-tjca-152*, https://de.nanotec.com/produkte/2736-lsa421s14-a-tjca-152, Mar. 2019.

[25] S. Lapin, K. Matveev, and M. Asle Zaeem, "The effect of vibration on flow rate of non-newtonian fluid," *Proceedings of SIAM Conference Mathematics for Industry 2009*, pp. 137–142, Apr. 2010. DOI: 10.1137/1.9781611973303.16.

[26] "Verfahren zur herstellung einer solarzelleneinrichtung," DE102021126772, 2023.

A. Appendix: Adhesive Data Sheets

WACKER® RTV-S 691 A/B

ELASTOSIL®

Room Temperature Curing Silicone Rubber (RTV-2)

WACKER® RTV-S 691 A/B is a self levelling, two-part addition curing silicone rubber which can be vulcanised at room temperature. Due to its low outgassing rate and low temperature flexibility it is recommended especially for space applications.
It has been designed and is used as adhesive for solar cells on solar generators for space applications such as satellites.

Properties

- resistant to low temperatures
- glass transition temperature: < -100 °C / -148 °F
- particularly low volatile contents
- admitted for aerospace applications by ESTEC (European Space Research and technology Centre) according to specification ECSS-Q-70-02A (corresponds to former ESA PSS-01-701)

Specific features

- Heat resistant
- Low volatile
- Low-temperature flexible
- UV stable

Technical data

Properties Uncured

Property	Condition	A	B	Method
Color	-	red	colourless, clear	-
Density	-	1.55 - 1.65 g/cm^3	0.98 g/cm^3	DIN EN ISO 2811-1
Viscosity, dynamic spindle 5, 2.5 rpm	23.0 °C	55000.0 - 70000.0 mPa·s	-	Brookfield
Viscosity	25 °C	-	200 - 240	ISO 3219

These figures are only intended as a guide and should not be used in preparing specifications.

Catalyzed

Property	Condition	Value	Method
Viscosity, dynamic (ca. 5 min after mixing the 2 components, shear rate 16 1/s)	23.0 °C	18000.0 - 26000.0 mPa·s	Brookfield
Mix ratio(1)	-	9 : 1	A : B
Pot life(2)	-	90 - 110 min	Brookfield

1(p.b.w.)
2(time to 200,000 mPa s at 16 1/s)

These figures are only intended as a guide and should not be used in preparing specifications.

Properties Cured

5 °C in press

Property	Condition	Value	Method
Density in water	23.0 °C	1.52 g/cm³	DIN EN ISO 1183-1 A
Hardness Shore A	-	50 - 60	DIN ISO 48-4
Tensile strength[1]	-	4.0 - 6.0 N/mm²	ISO 37
Elongation at break	-	100 - 160 %	ISO 37
Modulus at 100 % elongation elasticity	100.0 % | 23.0 °C | 50.0 % r. h	1.33 - 1.53 N/mm²	ISO 37
Volume resistivity	100.0 V | 1.0 min	> 1.0 x 10^{14} Ohmcm	IEC 62631-3-1
Surface resistivity	100.0 V	> 1.0 x 10^{12} OHM	-
Collected volatile condensable material CVCM [2]	-	< 0.1 %	-
Tear resistance	-	4.0 - 6.0 N/mm	ASTM D 624 B
Total mass loss TML	-	< 1.0 %	ESA ECSS-Q-70-02A

[1]ISO 37 Type 3
[2]ESA ECSS-Q-70-02A

These figures are only intended as a guide and should not be used in preparing specifications.

Applications

- Aerospace

Application details

Mixing ratio is 9:1 p.b.w Before taking component A out of the container or adding the catalyst, stir the material thoroughly. Components A and B can be mixed by hand or with metering equipment. The material must be evacuated before application to remove enclosed the bubbles. For detailed information refer to our leaflet "Wacker RTV-2 Silicone Rubber Processing". Important: The platinum catalyst is contained in component A. Caution! Only components A and B that have the same lot numer may be processed together! Mixing of the components It is ablolutely imperative that any equipment, such as mixing vessels, spatulas and stirres, that is used to process Component A (which contains the platinum catalyst) or the mixture of both components does not come into contact with Component B (which contains the crosslinker). Therefore, all equipment should be clearly labeled.

WACKER® RTV-S 691 A/B is used as silicone adhesive with minimum outgassing behaviour for space projects, e. g. bonding for solar cells in satellites.

RTV-S691 can be applied by silk screen printing or by dispensing equipment. In order to make the rubber adhere to other materials (e. g. glass, aluminium, silver, epoxy resin, polyester resin), it is necessary to pretreat the surface with Primer G 790.

Packaging and storage

Storage

The 'Best use before end' date of each batch is shown on the product label. Storage beyond the date specified on the label does not necessarily mean that the product is no longer usable. In this case however, the properties required for the intended use must be checked for quality assurance reasons.

Safety notes

Comprehensive instructions are given in the corresponding Material Safety Data Sheets. They are available on request from WACKER subsidiaries or may be printed via WACKER web site http://www.wacker.com.

QR Code WACKER® RTV-S 691 A/B

For technical, quality or product safety questions, please contact:

Wacker Chemie AG, Hanns-Seidel-Platz 4, 81737 Munich, Germany
info@wacker.com, www.wacker.com

B. Appendix: Component Data Sheets

30% Triple Junction GaAs Solar Cell Assembly

Type: TJ Solar Cell Assembly 3G30A

Improved Voltage at Maximum Power Point

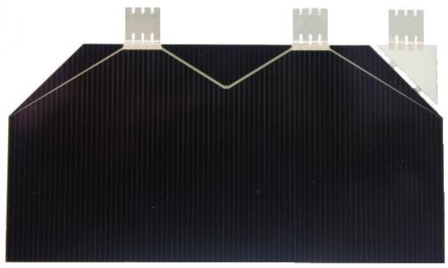

This cell type is a GaInP/GaAs/Ge on Ge substrate triple junction solar cell assembly (efficiency class 30%-Advanced). The solar cell assembly has an improved grid-design and is equipped with an external silicon bypass diode, interconnectors and cover glass.

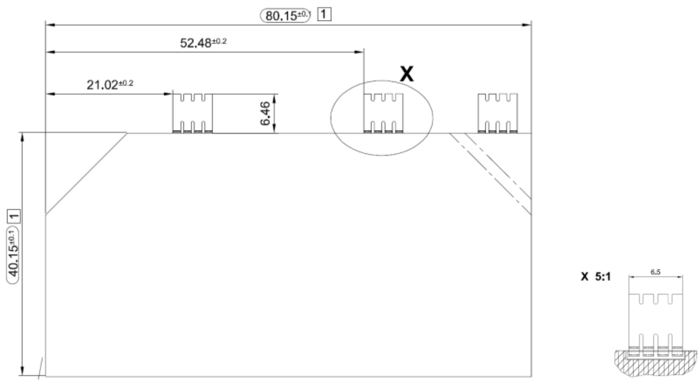

3G30A

AZUR SPACE Solar Power GmbH
Theresienstr. 2
74072 Heilbronn
phone: +49 7131 67 2603
telefax: +49 7131 67 2727
e-mail: info@azurspace.com
website: www.azurspace.de

Certified Company

ISO 9001
ISO 14001
OHSAS 18001

Space

30% Triple Junction GaAs Solar Cell Assembly
Type: TJ Solar Cell Assembly 3G30A

Design and Mechanical Data

Base Material	GaInP/GaAs/Ge on Ge substrate
AR-coating	TiO_x/Al_2O_3
SCA Dimensions	40.15 x 80.15 mm ± 0.1 mm
Cell Area	30.18 cm^2
SCA Average Weight	≤ 118 mg / cm^2
SCA Thickness	280 ± 25 µm
Coverglass type	CMX 100 AR
Coverglass thickness	100 µm
Interconnectors (2x front side/ 1x diode)	Kovar, silver coated
Dimensions (interconnector)	6.5 x 7.53 mm
Interconnector thickness	25 µm
Bypass protection	External Si diode

Electrical Data (SCA)

		BOL	2.5E14	5E14	1E15
Average Open Circuit V_{oc}	[mV]	2690	2606	2554	2512
Average Short Circuit I_{sc}	[mA]	519.6	517.9	513.4	501.3
Voltage at max. Power V_{mp}	[mV]	2409	2343	2288	2244
Current at max. Power I_{mp}	[mA]	502.9	501.7	499.1	485.1
Average Efficiency η_{bare} (1367 W/m^2)	[%]	29.3	28.4	27.6	26.3
Average Efficiency η_{bare} (1353 W/m^2)	[%]	29.6	28.7	27.9	26.6

Standard: CASOLBA 2005 (05-20MV1, etc); Spectrum: AMO WRC = 1367 W/m^2; T = 28 °C

@fluence 1MeV [e/cm²]

Acceptance Values (SCA)

Voltage V_{op}	2350 mV
Min. average current $I_{op\ avg}$ @ V_{op}	500 mA
Min. individual current $I_{op\ min}$ @ V_{op}	470 mA

Shadow protection

External Si protection diode T = 25°C ± 3°C	$V_{forward}$ (620 mA) ≤ 0.8 V $I_{reverse}$ (4V) ≤ 0.1 µA
Operation Temperatures	-150°C to +250°C

Temperature Gradients

			BOL	2.5E14	5E14	1E15
Open Circuit Voltage	$\Delta V_{oc}/\Delta T\uparrow$	[mV/°C]	- 6.2	- 6.5	- 6.6	- 6.7
Short Circuit Current	$\Delta I_{sc}/\Delta T\uparrow$	[mA/°C]	0.36	0.33	0.35	0.38
Voltage at max. Power	$\Delta V_{mp}/\Delta T\uparrow$	[mV/°C]	- 6.7	- 6.8	- 7.1	- 7.2
Current at max. Power	$\Delta I_{mp}/\Delta T\uparrow$	[mA/°C]	0.24	0.20	0.24	0.28

@fluence 1MeV [e/cm²]

Threshold Values

Absorptivity	≤ 0.91 (with CMX 100 AR)
Pull Test	> 7 N at 0° (with standard Kovar interconnector)

3G30A

Issue date:
2016-08-22

HNR 0003805-01-01

AZUR SPACE Solar Power GmbH
Theresienstr. 2
74072 Heilbronn
phone: +49 7131 67 2603
telefax: +49 7131 67 2727
e-mail: info@azurspace.com
website: www.azurspace.de

Certified Company

ISO 9001
ISO 14001
OHSAS 18001

Space

FRANKA EMIKA

PANDA - DATASHEET [1]

May 2019

HARDWARE

Arm

Degrees of freedom	7
Payload	3 kg
Workspace	see backside
Maximum reach	855 mm
F/T Sensing	link-side torque sensors in all 7 axes
Expected nominal lifetime [3,4]	20,000 h
Joint position limits [°]	A1, A3, A5, A7: -166/166 A2: -101/101 A4: -176/-4 A6: -1/215
Mounting flange	DIN ISO 9409-1-A50
Installation position	upright
Weight	~ 17.8 kg
Moving mass	~ 12.8 kg
Protection rating	IP30
Ambient temperature [2]	15 – 25 °C (typical) 5 – 45 °C (extended)
Air humidity	20 – 80 % non-condensing
Power consumption	• max. ~ 350 W • typical application ~ 60 W
Interfaces	• ethernet (TCP/IP) for visual intuitive programming with Desk • input for external enabling device • input for external activation device or safeguard • Control connector • Connector for end-of-arm tooling

Control

Controller size (19”)	355 x 483 x 89 mm (D x W x H)
Supply voltage	100 – 240 VAC
Mains frequency	47 – 63 Hz
Power consumption	~ 80 W
Active power factor correction (PFC)	yes
Weight	~ 7 kg
Protection rating	IP20
Ambient temperature	15 – 25 °C (typical) 5 – 45 °C (extended)
Air humidity	20 – 80 % non-condensing
Interfaces	• ethernet (TCP/IP) for internet and/or shop-floor connection • power connector IEC 60320-C14 (V-Lock) • Arm connector

SOFT-ROBOT PERFORMANCE

Motion

Joint velocity limits [°/s]	A1, A2, A3, A4: 150 A5, A6, A7: 180
Cartesian velocity limits	up to 2 m/s end effector speed
Pose repeatabillity	<+/- 0.1 mm (ISO 9283)
Path deviation [3]	<+/- 1.25 mm

Force

Sensing [3]

Force resolution	<0.05 N
Relative force accuracy	0.8 N
Force repeatability	<0.15 N
Force noise (RMS)	<0.035 N
Torque resolution	<0.02 Nm
Relative torque accuracy	0.15 Nm
Torque repeatability	<0.05 Nm
Torque noise (RMS)	<0.005 Nm

1 kHz Control [3]

Minimum controllable force (Fz)		0.05 N
Force controller bandwidth (-3 dB)		10 Hz
Force range [N]	Nominal case	Best case
Fx	-125 – 95	-150 – 115
Fy	-100 – 100	-275 – 275
Fz	-50 – 150	-115 – 155
Torque range [Nm]	Nominal case	Best case
Mx	-10 – 10	-70 – 70
My	-10 – 10	-16 – 12
Mz	-10 – 10	-12 – 12

Interaction

Guiding force	~ 2 N
Collision detection time	<2 ms
Nominal collision reaction time [3,4]	<50 ms
Worst case collision reaction time [3]	<100 ms
Adjustable translational stiffness	0 – 3000 N/m
Adjustable rotational stiffness	0 – 300 Nm/rad
Monitored signals	Joint position, velocity, torque Cartesian position, velocity, force

ADD-ONS

Safety retrofit option with safety-rated PLC	PLd Cat. 3 • Safe torque off (STO) • Safe OSSD inputs
Fully integrated end effectors	• 2-finger gripper • Vacuum gripper
Fast mounting	Paw
Demonstration	Pop-up Box
Research interface	1kHz Franka Control Interface
Fieldbuses	Modbus/TCP, OPC UA, Profinet

FRANKA EMIKA

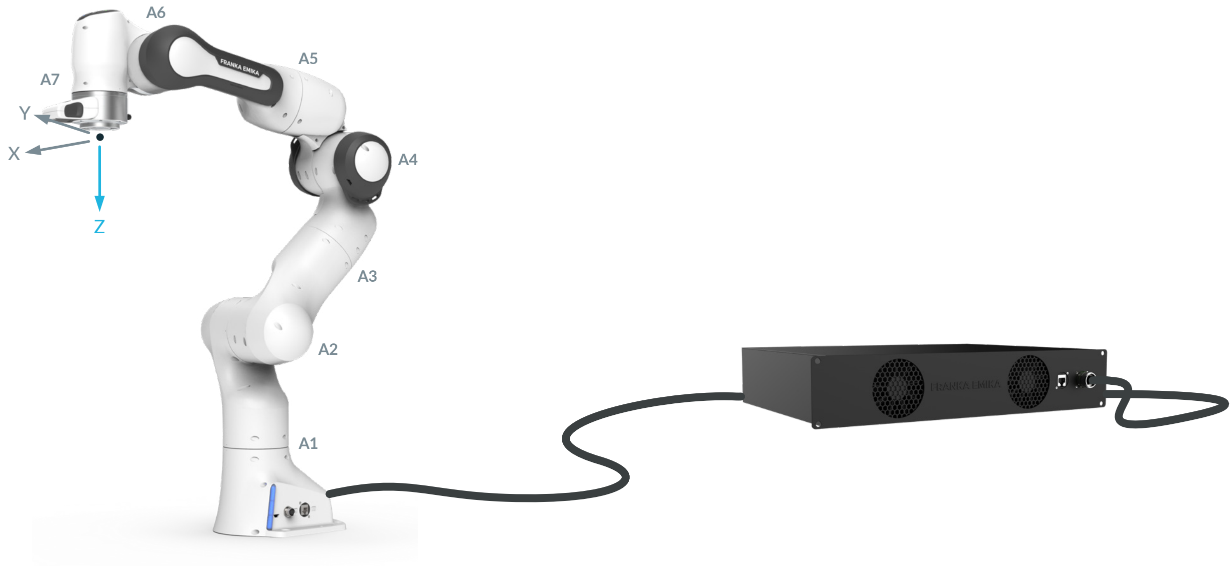

Arm & Control

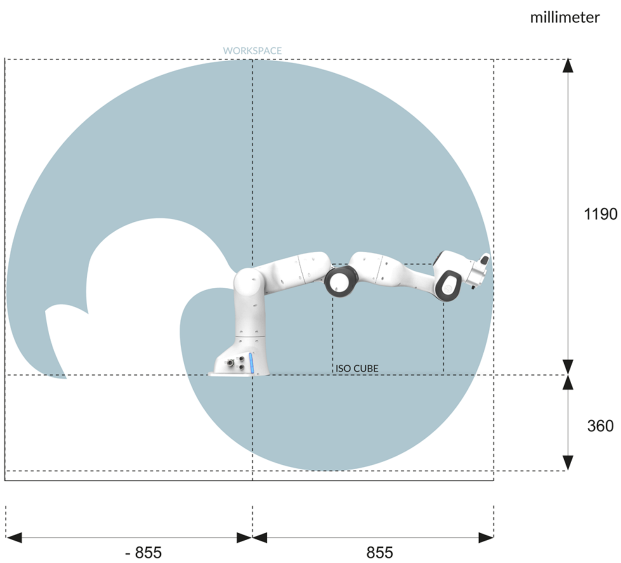

Workspace side-view

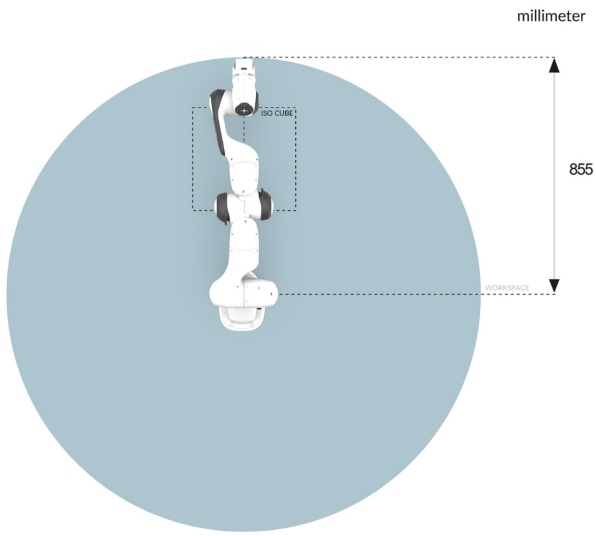

Workspace top-view

1. Technical data are subject to change.
2. Lifetime and performance can potentially be reduced when operating outside the typical temperature range.
3. Based on ISO 9283 (Annex A), specified values refer to a workspace of 0.4 x 0.4 x 0.4 m centered at [0.515, 0.0, 0.226] m, with the Z-Axis of the flange oriented parallel to earth-gravity and the elbow positioned upwards.
4. Nominal conditions (66% load).

Front view and mounting

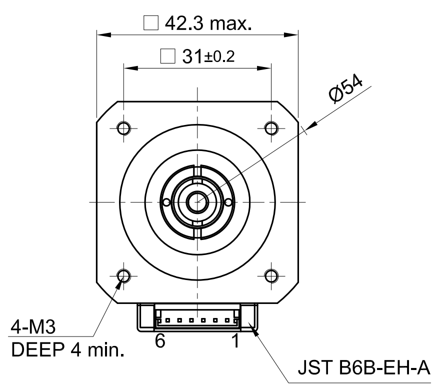

Side view

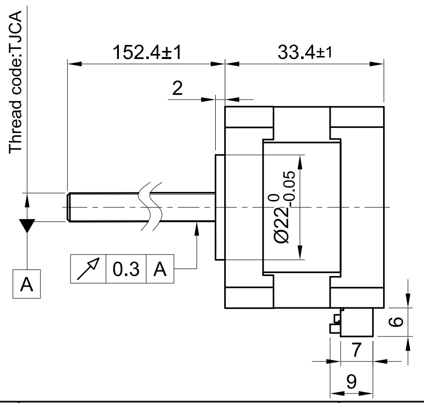

Rear view

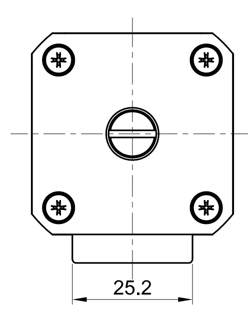

SPECIFICATION / CONNECTION	BIPOLAR
AMPS/PHASE	1.4
RESISTANCE/PHASE (Ohms)@25°C	2.0±15%
INDUCTANCE/PHASE (mH) @1KHz	2.8±20%
THREAD DIAMETER (mm) [in]	6 [0.236]
THREAD LEAD(mm) [in]	2 [0.078]
THRUST (N)	250
RESOLUTION (mm/STEP)	0.01
MAX. SPEED (mm/sec.) AT 24V	55
WEIGHT (Kg) [lb]	0.26 [0.57]
TEMPERATURE RISE: MAX.80°C (MOTOR STANDSTILL; FOR 2 PHASE ENERGIZED)	
AMBIENT TEMPERATURE −10°~ 50°C [14°F ~ 122°F]	
INSULATION RESISTANCE 100 MOhm (UNDER NORMAL TEMPERATURE AND HUMIDITY)	
INSULATION CLASS B 130° [266°F]	
DIELECTRIC STRENGTH 500VAC FOR 1 MIN. (BETWEEN THE MOTOR COILS AND THE MOTOR CASE)	
AMBIENT HUMIDITY MAX. 85% (NO CONDENSATION)	

Please regard the application note at www.nanotec.com for further informations.

MOTOR	
CONNECTOR PIN NO.	WINDING
1 (NC)	
2	A
3	A\
4	B
5	B\
6 (NC)	

FULL STEP 2 PHASE−Ex.,
WHEN FACING MOUNTING END (X)

STEP	A	B	A\	B\		CCW
1	+	+	−	−		
2	−	+	+	−		
3	−	−	+	+		
4	+	−	−	+	CW	

WIRING DIAGRAM

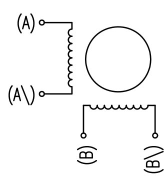

REV	DESCRIPTION	DATE	DRN							
				Nanotec® PLUG & DRIVE			APVD	P.R.	16.04.18	LINEAR ACTUATOR
B	−	13.03.19	X T				CHKD	GYQ	16.04.18	
A	−	13.08.18	X T	Surface specification DIN ISO 1302	General tolerances DIN ISO 2768-cH	Work piece edge DIN ISO 13715	DRN	X T	16.04.18	DWG.NO
REV	DESCRIPTION	DATE	DRN				SIGNATURE		DATE	LSA421S14−A−TJCA−152

C. Appendix: Bill of Material

Table C.1: bill of materials: dispensing tool

Pos-No.	Name	Description	QTY.
1	DIN 7991 - M3 x 12	Screw	4
2	DIN 7991 - M3 x 8	Screw	4
3	DIN 7991 - M5 x 16	Screw	8
4	DIN 912 M3 x 16	Screw	4
5	DIN 912 M5 x 20	Screw	2
6	DIN 912 M5 x 30	Screw	1
7	DIN 912 M3 x 10	Screw	4
8	DIN 912 M4 x 25	Screw	1
9	DIN 912 M3 x 12	Screw	8
10	Washer DIN 125	Washer	3
11	Washer DIN 125	Washer	12
12	Washer DIN 125	Washer	1
13	ISO - 4035 - M4	Nut	1
14	item Nutenstein_V_8_M5	Slot Nut	10
15	item_Profil_8_40x40x200	Item Aluminium Extrusion	1
16	SteperHalter_v03	3D-printed Part	1
18	SyringeConnector_03	3D-printed Part	1
19	NutSchlitten_v2	3D-printed Part	2
20	SwitchSupport_v02	3D-printed Part	1
21	ZIPPY-VA2	Limit Switch	1
22	KabelZugentlastungGr	3D-printed Part	1

Continued on next page

Table C.1: bill of materials: dispensing tool (Continued)

23	AdapterToolInterface_v2	3D-printed Part	1
24	Tool Interface 02	3D-printed Part	1
25	PistonConnectorTop	3D-printed Part	1
26	LSNUT-AAAE-TJCA	Nut for Lead Screw	1
27	PistonConnectorBottom	3D-printed Part	1
28	KabelZugentlastungMulti	3D-printed Part	1
29	Arduino Nano Every	Micro Controller	1
30	DRV8825	Stepper Driver	1
31	SN74HC595	Shift Register	1
32	ULN2803A	Transistor Array	1
33	DECA A20B-V4E02R	emergency off switch	1
34	TSR 2-2490	DC/DC Converter	1
35	Faber YSLY-JB 4 x 0.75 mm^2	Cable	2 m
36	ÖLFLEX 7G0,75	Cable	1 m
37	PTR 50350020001FV	Screw Terminal Block	13
38	100 µF Capacitor	Capacitor	2
39	100 nF Capacitor	Capacitor	2
40	LED	LED	6
41	220 Ω Resistor	Resistor	5
42	1 kΩ Resistor	Resistor	1
43	2 kΩ Resistor	Resistor	1
44	4.3 kΩ Resistor	Resistor	4
45	10 kΩ Resistor	Resistor	5
46	22 kΩ Resistor	Resistor	6
47	100 kΩ Resistor	Resistor	6

Table C.2: bill of materials: cell handling tool

Pos-No.	**Name**	**Discription**	**QTY.**
1	DIN 7991 - M4 x 12	Screw	16
2	DIN 912 M3 x 16	Screw	2
3	DIN 912 M6 x 20	Screw	1
4	Tool Interface 02	3D-printed Part	1
5	Vakuumgreifer_TraverseMitte_2mm_v2	3D-printed Part	1
6	MISUMI-Saugnapf-SRPF20	Suction Cup	10
7	DIN 912 M4 x 30	Screw	20
8	ISO - 4035 - M4	Nut	20
9	PannelSupport_v3	3D-printed Part	20
10	Vakuumgreifer_Traverse_2mm_v2	3D-printed Part	2
11	Adapter_v2	3D-printed Part	1